

Resummation of Large Endpoint Corrections to Color-Octet J/ψ Photoproduction

Sean Fleming^{*},¹ Adam K. Leibovich[†],² and Thomas Mehen[‡],^{3,4}

¹*Physics Department, University of Arizona, Tucson, AZ 85721*

²*Department of Physics and Astronomy,
University of Pittsburgh, Pittsburgh, PA 15260*

³*Department of Physics, Duke University, Durham, NC 27708*

⁴*Jefferson Laboratory, 12000 Jefferson Ave., Newport News, VA 23606*

(Dated: August 29, 2018)

Abstract

An unresolved problem in J/ψ phenomenology is a systematic understanding of the differential photoproduction cross section, $d\sigma/dz[\gamma + p \rightarrow J/\psi + X]$, where $z = E_\psi/E_\gamma$ in the proton rest frame. In the non-relativistic QCD (NRQCD) factorization formalism, fixed-order perturbative calculations of color-octet mechanisms suffer from large perturbative and nonperturbative corrections that grow rapidly in the endpoint region, $z \rightarrow 1$. In this paper, NRQCD and soft collinear effective theory are combined to resum these large corrections to the color-octet photoproduction cross section. We derive a factorization theorem for the endpoint differential cross section involving the parton distribution function and the color-octet J/ψ shape functions. A one loop matching calculation explicitly confirms our factorization theorem at next-to-leading order. Large perturbative corrections are resummed using the renormalization group. The calculation of the color-octet contribution to $d\sigma/dz$ is in qualitative agreement with data. Quantitative tests of the universality of color-octet matrix elements require improved knowledge of shape functions entering these calculations as well as resummation of the color-singlet contribution which accounts for much of the total cross section and also peaks near the endpoint.

^{*} Electronic address: fleming@physics.arizona.edu

[†] Electronic address: akl2@pitt.edu

[‡] Electronic address: mehen@phy.duke.edu

I. INTRODUCTION

Our current understanding of the production of heavy quarkonia is based on Non-Relativistic Quantum Chromodynamics (NRQCD) [1, 2, 3], an effective theory for bound states of two or more heavy quarks. The NRQCD factorization formalism solves important theoretical and phenomenological problems in quarkonium production and decay. Early color-singlet model calculations of χ_c decay were plagued by infrared divergences [4]. NRQCD solves this problem by providing a generalized factorization theorem which allows for infrared safe calculations of inclusive production and decay rates [5]. This formalism incorporates nonperturbative corrections to the color-singlet model, including color-octet decay and production mechanisms. Color-octet production mechanisms are necessary for understanding the production of J/ψ at large transverse momentum at the Fermilab Tevatron [6, 7]. However, the polarization of the observed J/ψ remains poorly understood [8].

The color-octet contribution to J/ψ photoproduction gives a large enhancement to the cross section near the kinematic endpoint defined by $z \rightarrow 1$, where $z = E_\psi/E_\gamma$ in the proton rest frame [9, 10]. Ref. [9] proposed that this peak constitutes a distinct signal for a color-octet contribution to photoproduction, and observed that such a signal is in contradiction with the experimental data which do not exhibit a peak. A crucial test of the NRQCD factorization theorem is verifying the universality of the color-octet matrix elements which enter into a variety of different J/ψ production processes, and the unobserved excess of J/ψ at the photoproduction endpoint could be interpreted as a failure of universality.

Color-octet matrix elements were first fit to hadroproduction data from the Tevatron [7], and have been refitted a number of times [11, 12, 13, 14] with general agreement among the various results. In general the extraction of the color-octet matrix elements has fairly large theoretical errors associated with it. The errors are particularly large on the extracted values of the color-octet matrix elements $\langle \mathcal{O}_8^{J/\psi}(^1S_0) \rangle$ and $\langle \mathcal{O}_8^{J/\psi}(^3P_J) \rangle$, which dominate the color-octet contribution to photoproduction, where a variation of almost an order of magnitude is typical. These large errors are thought to be due to higher order QCD corrections and as a result there has been an attempt to incorporate a subset of higher order contributions through the use of Monte Carlo methods [15] and a k_T factorization approach [16]. These approaches extract values for color-octet matrix elements up to 5 times smaller than the fixed-order calculations. Unfortunately, the rise in the fixed-order calculation of the color-octet photoproduction differential cross section is so dramatic that even the large uncertainties in the color-octet matrix elements cannot account for the discrepancy.

However, as one approaches the endpoint region, $z \rightarrow 1$, the fixed-order calculation of Refs. [9, 10] is invalidated by large perturbative and nonperturbative corrections. Specifically, perturbative corrections of the form

$$\alpha_s^n \frac{\ln^m(1-z)}{1-z}, \quad m \leq 2n - 1$$

are the source of the growth of the cross section as $z \rightarrow 1$ [17, 18]. These corrections must be resummed to all orders to make sensible comparison with data. There are also nonperturbative corrections scaling like $v^{2n}/(1-z)^n$, where v is the typical velocity of the $c\bar{c}$ within the J/ψ [19]. These corrections invalidate the NRQCD expansion near the kinematic endpoint. Ref. [20] addressed the latter issue by recalculating J/ψ photoproduction including a nonperturbative shape function which resums these corrections. The shape function tames perturbative endpoint divergences and results in a differential cross section that peaks near

$z \approx 0.9$. However, the peak in the differential cross section is too narrow to be compatible with data, and the authors conclude that a resummation of the singular perturbative contributions must also be carried out.

Similar issues arise when analyzing the production of J/ψ in e^+e^- collisions. In Ref.[21] a color-octet factorization theorem for $e^+ + e^- \rightarrow J/\psi + X$ was derived using a combination of NRQCD and soft collinear effective theory (SCET) [22, 23, 24, 25]. This approach resums nonperturbative and perturbative corrections that are enhanced near the kinematic endpoint. An important conclusion of Ref. [21] is that both the resummed perturbative corrections and the resummed non-perturbative corrections are necessary because the two effects act constructively to significantly broaden the spectrum.

In this paper we apply NRQCD and SCET to photoproduction at the endpoint of the spectrum. We derive a new factorization theorem for color-octet J/ψ photoproduction which resums endpoint corrections for this process. The factorization theorem in this case is more complicated than that for $e^+ + e^- \rightarrow J/\psi + X$ because there is a parton in the initial state hadron. To derive the factorization theorem, we first match QCD onto SCET_I (in which collinear partons have off-shellness $O(\sqrt{M\Lambda_{\text{QCD}}})$) at the scale $M = 2m_c$, and then match SCET_I onto SCET_{II} (where collinear partons have off-shellness $O(\Lambda_{\text{QCD}})$) [26] at an intermediate scale, $M\sqrt{1-z}$. At each stage we check that the effective field theory correctly reproduces the infrared physics of the previous theory to ensure that large logarithms are correctly resummed. Similarly, evolution of the renormalization group equations (RGE) is carried out in two stages. The first stage of evolution, from the scale M to the intermediate scale, $M\sqrt{1-z}$, is performed in SCET_I, while the second stage of evolution, from $M\sqrt{1-z}$ to $M(1-z)$, involves SCET_{II} running.

The factorization theorem is novel in that the J/ψ are not required to be produced with large transverse momentum, p_\perp , with respect to the photon-proton beam axis. Most perturbative analyses of J/ψ photoproduction assume that p_\perp of $O(1\text{ GeV})$ or larger is required for pQCD to be applicable to this process. For this reason, most phenomenological and experimental analyses impose a p_\perp cut on the data. Such a cut is inappropriate for application of the factorization theorem and the resummed cross sections derived in this paper.

Our final result for the color-octet contribution to $d\sigma/dz$ exhibits a spectrum that is significantly broadened and has a peak reduced in height relative to including only a shape function or only resumming the perturbative corrections, as anticipated. The inclusion of both nonperturbative and perturbative corrections significantly broadens the spectrum and is in qualitative agreement with data. However, fixed order color-singlet calculations are consistent with existing data on photoproduction so if these calculations are naively combined with our calculation, the color-octet matrix elements in photoproduction need to be roughly an order of magnitude smaller than those extracted from fixed-order analyses of Tevatron data. However, there are several sources of uncertainty which make it premature to attempt quantitative extraction of color-octet matrix elements using our calculation. Currently, the shape functions appearing in the photoproduction calculation have not been precisely determined. Also, consistency requires a similar resummation of endpoint effects in color-singlet photoproduction which accounts for much of the total photoproduction cross section. Finally, all of the existing data has cuts on p_\perp and/or cuts on diffractive contributions which are inappropriate for our analysis. Since the resummation is expected to suppress the color-singlet contribution, and the cuts tends to reduce the experimental cross section at largest values of z , a future analysis which takes these two effects into account

could find more room for a color-octet contribution.

This paper is organized as follows. In Section II, we derive the factorization theorem for the color-octet J/ψ photoproduction cross section near the endpoint, using the two-stage matching procedure discussed earlier. In Section III, we obtain analytic expressions for the leading logarithmically enhanced corrections at next-to-leading order (NLO) in QCD. In Section IV, we perform the matching calculations. This section is broken up into two subsections. In the first subsection we match the SCET_I current onto the QCD amplitude for $\gamma + g \rightarrow c\bar{c}$ at one loop and show that large logarithms are minimized at the scale M . In the second subsection we first calculate the NLO cross section in SCET_I. Correct evaluation of the SCET_I cross section requires care in avoiding the double counting of usoft modes and collinear modes with vanishing label momentum, the so-called “zero-bin” modes, as recently discussed in Ref. [27]. Taking this subtlety into account is necessary to demonstrate that SCET_I reproduces the large endpoint corrections of the NLO QCD calculation extracted in section III. We then match the SCET_I result onto SCET_{II}, which determines the intermediate matching scale. In Section V, we perform the RGE evolution which resums large perturbative corrections. In Section VI, we discuss the impact of the resummed color-octet differential cross section on the phenomenology of J/ψ photoproduction. A brief summary is provided in Section VII. Appendix A derives formulae that are useful for the extracting the large NLO corrections in Section III, and Appendix B provides some details about the zero-bin subtractions. Preliminary results describing some of the work here were presented at the Ringberg Workshop on New Trends in HERA Physics 2005 [28].

II. FACTORIZATION

In this section we derive a factorization theorem valid for J/ψ photoproduction near the kinematic endpoint, which is defined by $z \sim 1$, where $z = p_\psi \cdot p_P / p_\gamma \cdot p_P$, and p_ψ , p_P and p_γ are the four-momenta of the J/ψ , the initial state proton, and initial state photon, respectively. In the proton rest frame $z = E_\psi / E_\gamma$. We begin by showing that in the limit $z \rightarrow 1$, NRQCD factorization breaks down and SCET is required to obtain the appropriate factorization formula.

In the proton-photon center-of-mass frame

$$p_\gamma^\mu = \frac{\sqrt{s}}{2} \bar{n}^\mu, \quad p_P^\mu = \frac{\sqrt{s}}{2} n^\mu, \quad p_{c\bar{c}}^\mu = Mv^\mu + k^\mu, \quad (1)$$

where $s = (p_\gamma + p_P)^2$, $n^\mu = (1, 0, 0, -1)$, $\bar{n}^\mu = (1, 0, 0, 1)$, $M = 2m_c$, and v^μ and k^μ are the 4-velocity of the J/ψ and the residual momentum of the $c\bar{c}$ pair in the J/ψ , respectively. In terms of the scaling variable, z , the J/ψ velocity is

$$p_\psi^\mu = M_\psi v^\mu = \frac{z\sqrt{s}}{2} \bar{n}^\mu + p_\perp^\mu + \frac{m_\perp^2}{2z\sqrt{s}} n^\mu, \quad (2)$$

where $m_\perp^2 = M_\psi^2 + \mathbf{p}_\perp^2$. By momentum conservation we have

$$\begin{aligned} p_X^\mu &= p_\gamma^\mu + p_P^\mu - p_{c\bar{c}}^\mu \\ &= \frac{\sqrt{s}}{2} \left(1 - \frac{M}{M_\psi} z\right) \bar{n}^\mu + \frac{\sqrt{s}}{2} \left(1 - \frac{Mm_\perp^2}{szM_\psi}\right) n^\mu - \frac{M}{M_\psi} p_\perp^\mu - k^\mu. \end{aligned} \quad (3)$$

In NRQCD k^μ is typically dropped at lowest order, and terms with powers of k^μ are matched onto NRQCD operators with derivatives that are higher order in the v expansion. When the kinematics of a quarkonium production or decay process become sensitive to any components of k^μ such that this expansion breaks down, resummation of NRQCD operators into a shape function is required [19].

In the rest frame of the J/ψ all components of k^μ scale as Λ_{QCD} . In the proton-photon center-of-mass frame, the components of k^μ scale as

$$k^\mu = (n \cdot k, \bar{n} \cdot k, k_\perp) \sim \Lambda_{\text{QCD}} \left(\frac{z\sqrt{s}}{M}, \frac{M}{z\sqrt{s}}, 1 \right), \quad (4)$$

where we have neglected $O(p_\perp/\sqrt{s})$ corrections which are small in the endpoint region. The $n \cdot k$ component of k^μ is enhanced by \sqrt{s}/M , while the $\bar{n} \cdot k$ is suppressed by the same amount. Computing p_X^2 and keeping only the $n \cdot k$ component of k^μ we find

$$p_X^2 = s \left(1 - \frac{M}{M_\psi} z \right) \left(1 - \frac{Mm_\perp^2}{szM_\psi} \right) - \frac{M^2}{M_\psi^2} \mathbf{p}_\perp^2 - \sqrt{s} \left(1 - \frac{Mm_\perp^2}{szM_\psi} \right) n \cdot k + \dots \quad (5)$$

In the endpoint region, the transverse momentum of the J/ψ pair is of order $\sqrt{\hat{s}(1-z)} \sim \sqrt{\Lambda_{\text{QCD}}M} \sim 1 \text{ GeV}$, where $\sqrt{\hat{s}}$ is the *partonic* center-of-mass energy which is of order M in the endpoint region. Therefore, the term in Eq. (5) proportional to \mathbf{p}_\perp^2 is unimportant. Furthermore, for HERA kinematics, $\sqrt{s} \sim 100 \text{ GeV}$, so $Mm_\perp^2/(szM_\psi) \sim M^2/s \sim 10^{-3}$ for $z \approx 1$. The last term in Eq. (5) is as important as the first term when $n \cdot k \sim \sqrt{s}(1 - Mz/M_\psi)$, which occurs when $z \sim (M_\psi - \Lambda_{\text{QCD}})/M \sim 1$. In this region NRQCD factorization breaks down. From the point of view of SCET, a new factorization theorem is required when the final state particles recoiling against the J/ψ are jet-like and have to be described by SCET collinear fields rather than integrated out as in conventional NRQCD factorization. The final state is jet-like when $\bar{n} \cdot p_X \gg \sqrt{p_X^2}$, which is equivalent to $(1 - Mz/M_\psi) \ll 1$. This leads to the conclusion that as $z \rightarrow 1$, SCET is required for J/ψ photoproduction.

We derive the factorization formula for the photoproduction cross section in the endpoint region in two steps. First we match the QCD amplitude for $\gamma + g \rightarrow c\bar{c}$ onto the SCET_I current:

$$J^\mu(x) = \int d^3\boldsymbol{\omega} e^{i(Mv-\boldsymbol{\omega})\cdot x} C_\alpha^\mu(\boldsymbol{\omega}) J^\alpha(\boldsymbol{\omega}, x), \quad (6)$$

where

$$\int d^3\boldsymbol{\omega} \equiv \int d\bar{\omega} d^2\omega_\perp, \quad (7)$$

with $\boldsymbol{\omega}^\mu = \bar{\omega}n^\mu/2 + \omega_\perp^\mu$. The leading order contribution from the color-octet 1S_0 current is

$$J^\alpha(\boldsymbol{\omega}, x) = [\psi_{\mathbf{p}}^\dagger \delta^{(3)}(\vec{\mathcal{P}} - \boldsymbol{\omega}) B_\perp^\alpha \chi_{-\mathbf{p}}](x), \quad (8)$$

where B_\perp^α is the gauge invariant collinear gluon field defined by

$$B_\perp^\alpha = \frac{1}{g_s} W^\dagger (\mathcal{P}_\perp^\alpha + g_s (A_{n,q}^\alpha)_\perp) W,$$

and $\psi_{\mathbf{p}}$ and $\chi_{\mathbf{p}}$ are the NRQCD fields for the heavy quarks and antiquarks, respectively. The color-octet 3P_J current is

$$J_{\sigma\delta}^\alpha(\boldsymbol{\omega}, x) = \Lambda \cdot \hat{\mathbf{p}}_\sigma [\psi_{\mathbf{p}}^\dagger \Lambda \cdot \boldsymbol{\sigma}_\delta \delta^{(3)}(\vec{\mathcal{P}} - \boldsymbol{\omega}) B_\perp^\alpha \chi_{-\mathbf{p}}], \quad (9)$$

where $\widehat{\mathbf{p}}_\sigma = \Lambda_{i\sigma} p^i / M$, $\Lambda^{\mu\nu}$ is the boost matrix from the lab frame to the $c\bar{c}$ rest frame, and $\vec{\mathcal{P}}^\mu = \bar{\mathcal{P}} n^\mu / 2 + \mathcal{P}_\perp^\mu$ is the operator which projects out label momentum. We have defined

$$\delta^{(3)}(\vec{\mathcal{P}} - \boldsymbol{\omega}) \equiv \delta(\bar{\mathcal{P}} - \bar{\omega}) \delta^{(2)}(\mathcal{P}_\perp - \omega_\perp). \quad (10)$$

Tree level matching of QCD onto SCET_I determines the leading order Wilson coefficients for the $^1S_0^{(8)}$ and $^3P_J^{(8)}$ channels [21]:

$$\begin{aligned} C^{\mu\alpha}(^1S_0^{(8)}) &= \frac{-2ee_c g_s(M)}{M} \epsilon_\perp^{\mu\alpha}, \\ C^{\mu\alpha\delta\sigma}(^3P_J^{(8)}) &= \frac{-i4ee_c g_s(M)}{M} \left(g_\perp^{\alpha\delta} g_\perp^{\mu\sigma} + g_\perp^{\alpha\sigma} g_\perp^{\mu\delta} - g_\perp^{\alpha\mu} \bar{n}^\sigma \bar{n}^\delta \right). \end{aligned} \quad (11)$$

The second step is to match the differential cross section from SCET_I onto SCET_{II}. For clarity we will treat the $^1S_0^{(8)}$ contribution explicitly and state the final result for the $^3P_J^{(8)}$ channel. The SCET_I differential cross section is

$$\begin{aligned} 2E_\psi \frac{d\sigma}{d^3p_\psi} &= \int d^3\boldsymbol{\omega}_1 \int d^3\boldsymbol{\omega}_2 \frac{-C_{\beta\mu}^\dagger C_\alpha^\mu}{32\pi^3 s} \sum_{X_n, X_s} (2\pi)^4 \delta^{(4)}(p_\gamma + p_P - p_\psi - p_s - p_n) \\ &\times \frac{1}{2} \sum_{\text{spin}} \langle p_P | J^{\beta\dagger}(\boldsymbol{\omega}_1, 0) | J/\psi + X_s + X_n \rangle \langle J/\psi + X_s + X_n | J^\alpha(\boldsymbol{\omega}_2, 0) | p_P \rangle. \end{aligned} \quad (12)$$

where p_n is the total momentum of the final state collinear particles denoted by X_n , and p_s is the total momentum of the final state ultra-soft (usoft) particles, X_s . The momentum conserving delta function can be separated into light-cone coordinates:

$$\begin{aligned} \delta^{(4)}(p_\gamma + p_P - p_\psi - p_s - p_n) &= 2 \delta(\sqrt{s}(1-z) - n \cdot p_n - n \cdot p_s) \delta\left(\sqrt{s} \left(1 - \frac{m_\perp^2}{zs}\right) - \bar{n} \cdot p_n\right) \\ &\times \delta^{(2)}(p_\perp + p_{n\perp}), \end{aligned} \quad (13)$$

where p_\perp is the J/ψ transverse momentum. The usoft momentum is a subleading contribution in the last two terms on the right-hand-side and has been dropped. As pointed out earlier, in the endpoint region $|p_\perp| \ll M$ so from here on we let $m_\perp^2 \rightarrow M_\psi^2$.

We factor the collinear degrees of freedom from the soft through a field redefinition which decouples usoft and collinear fields in the SCET_I Lagrangian

$$B_\perp^\alpha(x) \rightarrow Y(x) B_\perp^{(0)\alpha}(x) Y^\dagger(x). \quad (14)$$

Here $Y(x)$ is a path ordered exponential of usoft gluon fields extending from $-\infty$ to x . The above field redefinition also shifts the collinear fields in the out state in such a way that $Y(x) \rightarrow \tilde{Y}(x)$ where $\tilde{Y}(x)$ is a path ordered exponential extending from x to ∞ [29]

$$\tilde{Y}(x) = \text{P exp} \left(ig \int_0^\infty ds n \cdot A_{us}(sn + x) \right). \quad (15)$$

As a consequence the matrix elements in Eq. (12) can be factored into separate collinear

and usoft pieces. The cross section in its factored form is

$$\begin{aligned}
2E_\psi \frac{d\sigma}{d^3p_\psi} &= \int d^3\omega_1 \int d^3\omega_2 \frac{-C_{\mu\beta}^\dagger C_\alpha^\mu}{32\pi^3 s} \sum_{X_n, X_s} 2(2\pi)^4 \delta(\sqrt{s}(1-z) - n \cdot p_n - n \cdot p_s) \\
&\times \delta\left(\frac{M_\psi^2}{z\sqrt{s}} - \bar{\omega}_2\right) \delta^{(2)}(p_\perp - \omega_{2\perp}) \\
&\times 2 \sum_{\text{spin}} \langle p_P | \text{Tr}[T^A B_\perp^\alpha(0)] \delta^{(3)}(\vec{\mathcal{P}}^\dagger - \omega_2) | X_n \rangle \langle X_n | \delta^{(3)}(\vec{\mathcal{P}} - \omega_1) \text{Tr}[T^B B_\perp^\beta(0)] | p_P \rangle \\
&\times \langle 0 | \chi_{-\mathbf{p}'}^\dagger \tilde{Y} T^A \tilde{Y}^\dagger \psi_{\mathbf{p}'}(0) | J/\psi + X_s \rangle \langle J/\psi + X_s | \psi_{\mathbf{p}}^\dagger \tilde{Y} T^B \tilde{Y}^\dagger \chi_{-\mathbf{p}}(0) | 0 \rangle, \quad (16)
\end{aligned}$$

where we have used conservation of the label momentum to replace the final state collinear momenta with ω and have dropped the (0) superscript on the collinear fields. The momentum components $n \cdot p_n \sim O(\Lambda_{\text{QCD}})$ are of the same size as the usoft momentum components. This remaining delta-function can be expressed as an integral over an exponential

$$(2\pi) \delta(\sqrt{s}(1-z) - n \cdot p_n - n \cdot p_s) = \int \frac{dx^-}{2} \exp\left[\frac{i}{2}(\sqrt{s}(1-z) - n \cdot p_n - n \cdot p_s)x^-\right], \quad (17)$$

which can be pulled into the factored matrix elements where it shifts fields from the origin to the point x^- . The explicit dependence on p_n and p_s disappears and the sums over final collinear and usoft states can be performed using completeness. Using $d^3p_\psi/(2E_\psi) = dzd^2p_\perp/(2z)$ gives

$$\begin{aligned}
\frac{d\sigma}{dzd^2p_\perp} &= \frac{-1}{16sz} \left(\frac{2ee_c g_s}{M}\right)^2 \int d^3\omega_+ \int \frac{dx^-}{2} e^{\frac{i}{2}\sqrt{s}(1-z)x^-} \delta\left(\frac{\bar{\omega}_+}{2} - \frac{M_\psi^2}{z\sqrt{s}}\right) \delta^{(2)}\left(p_\perp - \frac{\omega_{+\perp}}{2}\right) \\
&\times \frac{1}{2} \sum_{\text{spin}} \langle p_P | \text{Tr}[B_\perp^\nu(x^-) \delta^{(3)}(\vec{\mathcal{P}}_+ - \omega_+) B_{\perp\nu}(0)] | p_P \rangle \\
&\times \langle 0 | \chi_{-\mathbf{p}'}^\dagger \tilde{Y} T^A \tilde{Y}^\dagger \psi_{\mathbf{p}'}(x^-) \mathcal{P}_\psi \psi_{\mathbf{p}}^\dagger \tilde{Y} T^A \tilde{Y}^\dagger \chi_{-\mathbf{p}}(0) | 0 \rangle, \quad (18)
\end{aligned}$$

where we simplified the collinear matrix element by projecting onto a collinear operator in a color-singlet configuration. The expression above is further simplified by integrating over ω_+ and p_\perp

$$\begin{aligned}
\frac{d\sigma}{dz} &= \frac{-1}{8sz} \left(\frac{2ee_c g_s}{M}\right)^2 \int \frac{dx^-}{2} e^{\frac{i}{2}\sqrt{s}(1-z)x^-} \langle 0 | \chi_{-\mathbf{p}'}^\dagger \tilde{Y} T^A \tilde{Y}^\dagger \psi_{\mathbf{p}'}(x^-) \mathcal{P}_\psi \psi_{\mathbf{p}}^\dagger \tilde{Y} T^A \tilde{Y}^\dagger \chi_{-\mathbf{p}}(0) | 0 \rangle \\
&\times \frac{1}{2} \sum_{\text{spin}} \langle p_P | \text{Tr}[B_\perp^\nu(x^-) \delta\left(\vec{\mathcal{P}} - \frac{2M_\psi^2}{z\sqrt{s}}\right) B_{\perp\nu}(0)] | p_P \rangle, \\
&= \frac{-\pi}{2sz} \left(\frac{2ee_c g_s}{M}\right)^2 \langle \mathcal{O}_8^{J/\psi}(^1S_0) \rangle M \int dk^+ S^{(8,^1S_0)}(-\sqrt{s}(1-z) + k^+) \mathcal{J}_P(k^+). \quad (19)
\end{aligned}$$

The cross section is expressed as a convolution of a shape function, $S^{(8,^1S_0)}$, and a jet function, \mathcal{J}_P , that are defined as follows:

$$S^{(8,^1S_0)}(\ell^+) \equiv \int \frac{dx^-}{4\pi} e^{-\frac{i}{2}\ell^+ x^-} \frac{\langle 0 | \chi_{-\mathbf{p}'}^\dagger \tilde{Y} T^A \tilde{Y}^\dagger \psi_{\mathbf{p}'}(x^-) \mathcal{P}_\psi \psi_{\mathbf{p}}^\dagger \tilde{Y} T^A \tilde{Y}^\dagger \chi_{-\mathbf{p}}(0) | 0 \rangle}{2M \langle \mathcal{O}_8^{J/\psi}(^1S_0) \rangle}, \quad (20)$$

$$\mathcal{J}_P(k^+) \equiv \int \frac{dy^-}{4\pi} e^{\frac{i}{2}k^+y^-} \frac{1}{2} \sum_{\text{spin}} \langle p_P | \text{Tr} [B_{\perp}^{\nu}(y^-) \delta\left(\bar{\mathcal{P}} - \frac{2M_{\psi}^2}{\sqrt{s}}\right) B_{\perp\nu}(0)] | p_P \rangle. \quad (21)$$

We have set $z \rightarrow 1$ inside the matrix element in the definition of the jet function since the matrix element is smooth as $z \rightarrow 1$ and leads to no large logs. We will also set $z \rightarrow 1$ in the prefactor of the cross section appearing in Eq. (19). The shape function is normalized so that $\int dk^+ S^{(8,1S_0)}(k^+) = 1$.

Taking moments of the cross section with respect to z , $\sigma_N \equiv \int_0^1 dz z^N d\sigma/dz$, and considering the large N limit, we will see below that σ_N is the product of moments of the shape function and jet function. Large logs of M/N are contained in moments of the shape function and large logs of M/\sqrt{N} are contained in the moments of \mathcal{J}_P , so the two scales are separated in Eq. (19). However, the jet function still depends two scales, the perturbative scale, M/\sqrt{N} , as well as the long distance scale, Λ_{QCD} . Dependence on the latter scale arises because the matrix element is taken between proton states. In this respect, the jet function that appears in Eq. (19) is quite different from the perturbatively calculable jet function that appears in the endpoint resummation of $e^+ + e^- \rightarrow J/\psi + X$ [21].

Since the jet function, \mathcal{J}_P , contains both perturbative and nonperturbative scales, we can perform a further factorization on this matrix element. Because the external gluons in the proton have off-shellness $O(\Lambda_{\text{QCD}})$, the matrix element should be evaluated in SCET_{II} rather than SCET_I. The factorization can be thought of as arising from matching the nonlocal SCET_I operator in Eq. (21) onto local operators in SCET_{II}. Intuitively we expect the result to be a convolution of short distance coefficient which is perturbatively calculable and contains large logarithms of M/\sqrt{N} with a parton distribution function for the gluon in the proton.

To demonstrate this we define the variable, $\rho = M_{\psi}^2/s$, and take moments of \mathcal{J}_P with respect to ρ :

$$\begin{aligned} \int_0^1 d\rho \rho^N \mathcal{J}_P(k^+) &= \int_0^1 d\rho \rho^N \int \frac{dy^-}{4\pi} e^{\frac{i}{2}k^+y^-} \\ &\quad \times \frac{1}{2} \sum_{\text{spin}} \langle p_P | \text{Tr} [B_{\perp}^{\nu}(y^-) \delta(\bar{\mathcal{P}} - 2\rho\sqrt{s}) B_{\perp\nu}(0)] | p_P \rangle \\ &= \int \frac{dy^-}{4\pi} e^{\frac{i}{2}k^+y^-} \frac{1}{2} \sum_{\text{spin}} \langle p_P | \text{Tr} [B_{\perp}^{\nu}(y^-) \frac{\bar{\mathcal{P}}^N}{(2\sqrt{s})^{N+1}} B_{\perp\nu}(0)] | p_P \rangle. \end{aligned} \quad (22)$$

Now we apply the operator product expansion (OPE) to the matrix element, which is justified when matching onto SCET_{II} because the momentum $k^+ \sim O(M/\sqrt{N})$ is parametrically larger than Λ_{QCD} :

$$\begin{aligned} \int_0^1 d\rho \rho^N \mathcal{J}_P(k^+) &= \int \frac{dy^-}{4\pi} e^{\frac{i}{2}k^+y^-} C(N, y^-) \frac{1}{2} \sum_{\text{spin}} \langle p_P | \text{Tr} [B_{\perp}^{\nu} \frac{\bar{\mathcal{P}}^N}{(2\sqrt{s})^{N+1}} B_{\perp\nu}] | p_P \rangle \\ &= -\frac{1}{4s} \tilde{C}(N, k^+) \int_0^1 d\xi \xi^{N-1} f_{g/P}(\xi), \end{aligned} \quad (23)$$

where

$$\tilde{C}(N, k^+) = \sqrt{s} \int \frac{dy^-}{4\pi} e^{\frac{i}{2}k^+y^-} C(N, y^-), \quad (24)$$

is dimensionless. Therefore the moments of the jet function are proportional to the moments of the structure function for the gluon in the proton, whose definition in SCET is [30]

$$\frac{1}{2} \sum_{\text{spin}} \langle p_P | [\text{Tr}\{B_{\perp}^{\nu}(0)\delta(\bar{\mathcal{P}}_+ - \bar{\omega}_+)B_{\perp\nu}(0)\}] | p_P \rangle = -\frac{1}{2\bar{\omega}_+} f_{g/P} \left(\frac{\bar{\omega}_+}{2\bar{n} \cdot p_P} \right). \quad (25)$$

The result in Eq. (23) is easily seen to be equivalent to the following convolution:

$$\mathcal{J}_P(k^+) = \frac{-1}{4\rho s} \int_{\rho}^1 \frac{d\xi}{\xi} C_{II} \left(\frac{\rho}{\xi}, k^+ \right) f_{g/P}(\xi), \quad (26)$$

where the function $C_{II}(\rho/\xi, k^+)$ can be obtained from the coefficients in the OPE, $\tilde{C}(N, k^+)$, by inverse Mellin transform. The resulting expression for the cross section is

$$\frac{d\sigma}{dz} = \sigma_0 \rho \int dk^+ S^{(8,1S_0)}(-\sqrt{s}(1-z) + k^+) \int_{\rho}^1 \frac{d\xi}{\xi} C_{II} \left(\frac{\rho}{\xi}, k^+ \right) f_{g/P}(\xi), \quad (27)$$

where

$$\sigma_0 = \frac{\pi^3 \alpha \alpha_s e_c^2}{4m_c^5} \langle \mathcal{O}_8^{J/\psi}(1S_0) \rangle,$$

and we have set $\rho = 4m_c^2/s$. The factorized form for the color-octet P-wave contribution to the cross section is obtained by making the replacement

$$\langle \mathcal{O}_8^{J/\psi}(1S_0) \rangle \rightarrow \frac{7}{m_c^2} \langle \mathcal{O}_8^{J/\psi}(3P_0) \rangle, \quad (28)$$

and replacing $S^{(8,1S_0)}$ with $S^{(8,3P_0)}$. The shape functions in each channel are normalized the same way. Eq. (27) is modified once higher order corrections to the matching coefficients in Eq. (11) are included. We parametrize these corrections as follows:

$$C^{\mu\alpha}(1S_0^{(8)}) = C_V(\bar{\mu}) \frac{-2ee_c g_s(M)}{M} \epsilon_{\perp}^{\mu\alpha} \quad (29)$$

and similarly for $3P_J^{(8)}$ channels. Including these corrections gives the final form of the factorization theorem:

$$\frac{d\sigma}{dz} = \sigma_0 \rho |C_V(\bar{\mu})|^2 \int dk^+ S^{(8,1S_0)}(-\sqrt{s}(1-z) + k^+) \int_{\rho}^1 \frac{d\xi}{\xi} C_{II} \left(\frac{\rho}{\xi}, k^+ \right) f_{g/P}(\xi). \quad (30)$$

This factorization theorem for endpoint photoproduction of J/ψ is the main result of this paper. For the remainder of this section we set $C_V(\bar{\mu}) = 1$. In section V, where large logarithms are resummed, an important step is evolving $C_V(\bar{\mu})$ from the scale $\bar{\mu} = M$, where QCD is matched onto SCET_I, to the scale $\bar{\mu} = M/\sqrt{N}$, where SCET_I is matched onto SCET_{II}.

Our result should reproduce previous results for photoproduction in the appropriate limits. To lowest order in α_s the coefficients in the OPE are $C(N, y^-) = 1$, which is equivalent to

$$C_{II} \left(\frac{\rho}{\xi}, k^+ \right) = \sqrt{s} \delta(k^+) \delta \left(1 - \frac{\rho}{\xi} \right). \quad (31)$$

Inserting this into Eq. (27) yields

$$\frac{d\sigma}{dz} = \frac{\pi^3 \alpha \alpha_s e_c^2}{sm_c^3} \langle \mathcal{O}_8^{J/\psi}(^1S_0) \rangle \sqrt{s} S^{(8,^1S_0)}(-\sqrt{s}(1-z)) f_{g/P}(\rho). \quad (32)$$

To lowest order in v^2 , $\sqrt{s} S^{(8,^1S_0)}(-\sqrt{s}(1-z)) \rightarrow \delta(1-z)$ which is easily seen to reproduce the tree level calculation of Ref. [31].

Finally, it is useful to derive an expression for the moments of the cross section. Defining $k^+ = \sqrt{s}(u-z)$, the normalized differential cross section is

$$\frac{1}{\sigma_0} \frac{d\sigma}{dz} = \rho \int_z^1 du \hat{S}^{(8,^1S_0)}(u) \int_\rho^1 \frac{d\xi}{\xi} C_{II} \left(\frac{\rho}{\xi}, u-z \right) f_{g/P}(\xi), \quad (33)$$

where $\hat{S}^{(8,^1S_0)}(u) = \sqrt{s} S^{(8,^1S_0)}(-\sqrt{s}(1-u))$ and we have rescaled second argument of C_{II} . It is now straightforward to take moments of the cross section and show that, for large N , the normalized moments of the cross section factorize:

$$\frac{\sigma_N}{\sigma_0} \equiv \frac{1}{\sigma_0} \int_0^1 dz z^N \frac{d\sigma}{dz} = \rho \tilde{S}^{(8,^1S_0)}(N) \int_\rho^1 \frac{d\xi}{\xi} \hat{C}_{II} \left(\frac{\rho}{\xi}, N \right) f_{g/P}(\xi), \quad (34)$$

where

$$\begin{aligned} \tilde{S}^{(8,^1S_0)}(N) &= \int_0^1 du u^N \hat{S}^{(8,^1S_0)}(u), \\ \hat{C}_{II} \left(\frac{\rho}{\xi}, N \right) &= \int_0^1 dz z^N C_{II} \left(\frac{\rho}{\xi}, 1-z \right). \end{aligned} \quad (35)$$

We will show in Sec. IV that the moments of the QCD cross section at lowest nontrivial order factorize in a manner consistent with Eq. (34), providing additional evidence for the factorization theorem.

III. EXTRACTING LARGE LOGS AT NLO

A calculation of the leading color-octet contribution to the forward cross section for J/ψ photoproduction appeared in Ref. [31]. The NLO calculation of the color-octet contribution to $d\sigma/dz$, $z \neq 1$, was carried out in Refs. [9, 13], but these papers presented only numerical results. Refs. [10, 32] presented analytic results for the total partonic cross section. In this section we obtain analytic expressions for the leading logarithmically enhanced corrections to the color-octet differential cross section in NRQCD. By logarithmically enhanced we mean corrections of the form:

$$\frac{1}{\sigma_0} \frac{d\hat{\sigma}[\gamma + g \rightarrow J/\psi + X]}{dz} \propto \alpha_s \left(\frac{\ln(1-z)}{1-z} \right)_+, \alpha_s \left(\frac{1}{1-z} \right)_+. \quad (36)$$

When moments of the cross section are taken, $\int_0^1 dz z^N d\sigma/dz$, the distributions in Eq. (36) give rise to terms $\propto \alpha_s \ln^2 N$ and $\alpha_s \ln N$, respectively. These are the logarithmically enhanced terms we wish to resum to all orders in perturbation theory. Terms in the differential cross section less singular in $1-z$ give contributions to the moments which are suppressed by

powers of N , e.g. $\int_0^1 dz z^N \ln(1-z) = \ln \bar{N}/N + O(1/N^2)$, where $\bar{N} = Ne^{\gamma_E}$, and will be ignored.

The analytic result for the logarithmically enhanced corrections is helpful for checking our factorization theorem for the resummed cross section. Furthermore, in our derivation of the factorization theorem, QCD currents are first matched onto SCET_I operators, then the cross section in SCET_I is matched onto SCET_{II}. In both matching calculations, we wish to verify that no large logarithms appear in the matching coefficients so we are sure that large logarithms are properly resummed using the RGEs. The condition that the large logs cancel in the matching from SCET_I and SCET_{II} determines the scale at which SCET_I is matched onto SCET_{II}.

The hadronic cross section is obtained by convoluting the partonic cross section with a parton distribution function (pdf):

$$\frac{d\sigma[\gamma + P \rightarrow J/\psi + X]}{dz} = \sum_i \int_\rho^z dx \frac{\rho}{x^2} f_{i/P} \left(\frac{\rho}{x} \right) \frac{d\hat{\sigma}[\gamma + i \rightarrow J/\psi + X]}{dz}. \quad (37)$$

Here $\rho = M^2/s$ and $x = M^2/\hat{s}$, where \hat{s} is the center of mass energy squared in the partonic collision. There is a sum over parton species, i , and $f_{i/P}$ is the pdf for the proton. For the rest of the paper we will restrict ourselves to the dominant production process which is initiated by a gluon. In the HERA collider J/ψ photoproduction experiments $\sqrt{s} \sim 100$ GeV so $\rho \approx 10^{-3}$. Though we cannot set ρ to zero inside the argument of the pdf, we can set $\rho = 0$ in the limit of the x integration since the logarithmically enhanced terms come from the opposite end of the integral. Calculation of the partonic cross section is simplified by making this approximation, so we will use the standard distributional identity

$$(1-x)^{-1-\epsilon} = -\frac{1}{\epsilon} \delta(1-x) + \left(\frac{1}{1-x} \right)_+ - \epsilon \left(\frac{\ln(1-x)}{1-x} \right)_+ + O(\epsilon^2), \quad (38)$$

instead of [32]

$$(1-x)^{-1-\epsilon} = -\frac{\beta^{-2\epsilon}}{\epsilon} \delta(1-x) + \left(\frac{1}{1-x} \right)_\rho - \epsilon \left(\frac{\ln(1-x)}{1-x} \right)_\rho + O(\epsilon^2), \quad (39)$$

where $\beta = \sqrt{1-\rho}$ and the ρ -distributions are defined by

$$\int_\rho^1 dx [t(x)]_\rho f(x) = \int_\rho^1 dx t(x) [f(x) - f(1)]. \quad (40)$$

By using Eq. (38) rather than Eq. (39) we omit corrections proportional to $\log \beta \sim 10^{-3}$ which can be safely neglected.

The leading order contribution to the production of J/ψ via color-octet mechanisms is the two-to-one process, $\gamma g \rightarrow c\bar{c}^{(8)}(^{2S+1}L_J)$, where one of the two Feynman diagrams is depicted in Fig. 1. This gives a contribution to the partonic cross section [31]

$$\begin{aligned} \frac{d\hat{\sigma}^{\text{LO}}}{dz} &= \frac{\pi^3 \alpha_s \alpha e_c^2}{4m_c^5} \left[\langle \mathcal{O}_8^{J/\psi}(^1S_0) \rangle + \frac{7}{m_c^2} \langle \mathcal{O}_8^{J/\psi}(^3P_0) \rangle \right] \delta(1-x) \delta(1-z) \\ &\equiv \sigma_0 \delta(1-x) \delta(1-z). \end{aligned} \quad (41)$$

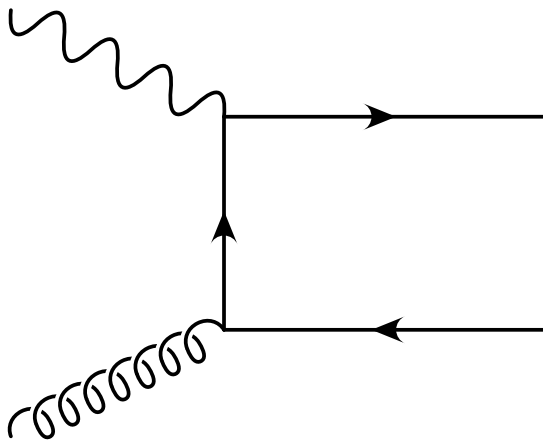


FIG. 1: One of two leading order QCD diagram for $\gamma g \rightarrow c\bar{c}^{(8)}(^{2S+1}L_J)$. The other Feynman graph is obtained by reversing the direction of the fermion line

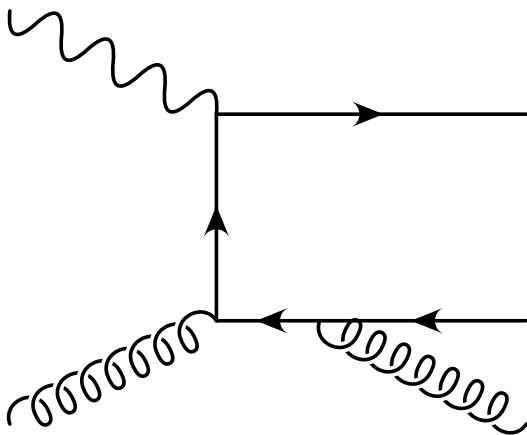


FIG. 2: An example of a NLO QCD diagram contributing to photoproduction.

An example of a next-to-leading order real emission diagram that contributes to the photoproduction cross section for $z \neq 1$ is shown in Fig. 2. It is these graphs that contribute the large logarithms at NLO we wish to resum. Infrared (IR) divergences in these graphs will be regulated using dimensional regularization and the IR divergences are cancelled by virtual corrections to the LO graphs, Fig. 1, or by the parton distribution function.

The partonic cross section obtained from summing all the NLO real emission diagrams in the color-octet 1S_0 channel is

$$\frac{d\hat{\sigma}^{\text{real}}}{dz} = \sigma_0 \frac{C_A \alpha_s}{\pi} \left(\frac{4\pi\mu^2}{M^2} \right)^\epsilon \frac{x^\epsilon (1-z)^{-\epsilon} (z-x)^{-\epsilon}}{\Gamma[1-\epsilon]} \mathcal{M}(x, z), \quad (42)$$

where

$$\mathcal{M}(x, z) = \frac{x^2(z-x)[(1-z+z^2)^2 + x(x-z)(x(x-z) + 2z^2)]}{(1-x)^2(1+x-z)^2(1-z)z^2}. \quad (43)$$

The phase space is in $D = 4 - 2\epsilon$ dimensions. The logarithmically enhanced terms come from the limit $z \rightarrow 1$. Expanding $M(x, z)$ about $z = 1$ we find

$$\mathcal{M}(x, z) = \frac{(1-x+x^2)^2}{(1-x)(1-z)} + \frac{-2+5x-6x^2+5x^3-6x^4+5x^5-2x^6}{x(1-x)^2} + O(1-z). \quad (44)$$

Terms $O(1-z)$ and higher do not give logarithmically enhanced contributions, even after performing the x integration, and therefore can be dropped. Furthermore,

$$\int^z dx \frac{1}{(1-x)^2} \propto \frac{1}{1-z} \quad \int^z dx \frac{1}{(1-x)} \propto \ln(1-z), \quad (45)$$

so terms proportional to $1/(1-x)^2$ give logarithmically enhanced corrections while terms proportional to $1/(1-x)$ can be dropped. Thus the second term on the right hand side of Eq. (44) can be expanded around $x = 1$,

$$\begin{aligned} \frac{d\hat{\sigma}^{\text{real}}}{dz} &= \sigma_0 \frac{C_A \alpha_s}{\pi} \left(\frac{4\pi\mu^2}{M^2} \right)^\epsilon \frac{x^\epsilon(1-z)^{-\epsilon}(z-x)^{-\epsilon}}{\Gamma[1-\epsilon]} \left[\frac{(1-x+x^2)^2}{(1-x)(1-z)} - \frac{1}{(1-x)^2} + \dots \right] \\ &= \sigma_0 \frac{\alpha_s}{2\pi} \left(\frac{4\pi\mu^2}{M^2} \right)^\epsilon \frac{x^\epsilon(1-z)^{-\epsilon}(z-x)^{-\epsilon}}{\Gamma[1-\epsilon]} \left[\frac{xP_{gg}(x)}{1-z} - \frac{2C_A}{(1-x)^2} + \dots \right], \end{aligned} \quad (46)$$

where the ellipsis represents terms that do not give logarithmically enhanced corrections and $P_{gg}(x)$ is the related to the real emission part of the gluon splitting function:

$$P_{gg}(x) = 2C_A \left[\frac{x}{1-x} + \frac{1-x}{x} + x(1-x) \right].$$

The gluon splitting function, $\mathcal{P}_{gg}(x)$, will appear in what follows and is defined by:

$$\begin{aligned} \mathcal{P}_{gg}(x) &= \bar{P}_{gg}(x) + b_0 \delta(1-x), \\ \bar{P}_{gg}(x) &= 2C_A \left[\frac{x}{(1-x)_+} + \frac{1-x}{x} + x(1-x) \right], \\ b_0 &= \frac{11}{6}C_A - \frac{2}{3}T_F n_f. \end{aligned} \quad (47)$$

In Eq. (46) the first term in square brackets contains the collinear divergence, as is easily seen by noting that $1-z = (1-x)(1-\cos\theta)/2$, where $\cos\theta$ is the angle between initial and final state gluon momentum in the parton center of mass frame.

Though we have derived Eq. (46) for the 1S_0 channel, the result is in fact universal and holds for the color-octet channels $^1S_0, ^3P_{0,2}$ regardless of the angular momentum quantum numbers of the final state $c\bar{c}$. QCD factorization theorems guarantee that the term with the $1/(1-z)$ pole in the real emission cross section has the same form for all color-octet production channels. The universality of the double pole, $1/(1-x)^2$, is verified by calculating QCD diagrams in the soft gluon approximation, which is valid in the limit $x \rightarrow 1$ [32].

To obtain the logarithmically enhanced corrections we need to perform the integration over x . At first sight, deriving an analytic expression appears to be difficult since the pdf contains x dependence which is not known in closed form. However, it is possible to extract the leading corrections analytically using the following distributional identities, derived in Appendix A:

$$\begin{aligned}
(1-z)^{-1-\epsilon} \int_0^z dx \frac{(z-x)^{-\epsilon}}{1-x} g(x) &= \tag{48} \\
\delta(1-z) \left[\left(\frac{1}{2\epsilon^2} - \frac{\pi^2}{12} \right) g(1) - \frac{1}{\epsilon} \int_0^1 dx \left(\frac{1}{1-x} \right)_+ g(x) + \int_0^1 dx \left(\frac{\ln(1-x)}{1-x} \right)_+ g(x) \right] \\
+ \left(\frac{1}{1-z} \right)_+ \int_0^1 dx \left(\frac{1}{1-x} \right)_+ g(x) - g(1) \left(\frac{\ln(1-z)}{1-z} \right)_+ , \\
\int_0^z dx \frac{(z-x)^{-\epsilon} (1-z)^{-\epsilon}}{(1-x)^2} g(x) &= \left[-\frac{1}{2\epsilon} \delta(1-z) + \left(\frac{1}{1-z} \right)_+ \right] g(1), \tag{49}
\end{aligned}$$

where $g(x)$ is arbitrary. On the right hand side we only keep terms proportional to singular distributions in $1-z$. This includes the singular distributions in Eq. (36) which contribute to the large logarithms in moment space as well as terms proportional to $\delta(1-z)$. These terms contain IR divergences which cancel against virtual graphs or are absorbed into the pdf.

The NLO result for the part of the partonic real emission contribution to $d\sigma/dz$ that is singular as $z \rightarrow 1$ is

$$\begin{aligned}
\frac{d\hat{\sigma}^{\text{real}}}{dz} &= \sigma_0 \frac{C_A \alpha_s}{\pi} \times \tag{50} \\
&\left(\delta(1-z) \left\{ \delta(1-x) \left[\frac{1}{2\epsilon^2} + \frac{1}{2\epsilon} + \frac{1}{2\epsilon} \ln \left(\frac{\bar{\mu}^2}{M^2} \right) + \frac{1}{2} \ln \left(\frac{\bar{\mu}^2}{M^2} \right) + \frac{1}{4} \ln^2 \left(\frac{\bar{\mu}^2}{M^2} \right) - \frac{\pi^2}{8} \right] \right. \right. \\
&\quad \left. \left. + (1-x+x^2)^2 \left[\left(-\frac{1}{\epsilon} - \ln \left(\frac{\bar{\mu}^2 x}{M^2} \right) \right) \left(\frac{1}{1-x} \right)_+ + \left(\frac{\ln(1-x)}{1-x} \right)_+ \right] \right\} \right. \\
&\quad \left. + \left(\frac{1}{1-z} \right)_+ \left[-\delta(1-x) + (1-x+x^2)^2 \left(\frac{1}{1-x} \right)_+ \right] - \delta(1-x) \left(\frac{\ln(1-z)}{1-z} \right)_+ \right),
\end{aligned}$$

where we define $\bar{\mu}^2 = 4\pi\mu^2 e^{-\gamma_E}$. If we take moments of this cross section with respect to the variable z we find

$$\begin{aligned}
\frac{\hat{\sigma}_N^{\text{real}}}{\sigma_0} &= \delta(1-x) \frac{C_A \alpha_s}{\pi} \times \tag{51} \\
&\left[\frac{1}{2\epsilon^2} + \frac{1}{2\epsilon} + \frac{1}{2\epsilon} \ln \left(\frac{\bar{\mu}^2}{M^2} \right) + \frac{1}{4} \ln^2 \left(\frac{\bar{\mu}^2}{M^2} \right) + \frac{1}{2} \ln \left(\frac{\bar{\mu}^2}{M^2} \right) + \ln(\bar{N}) - \frac{1}{2} \ln^2(\bar{N}) - \frac{\pi^2}{8} \right] \\
&+ \frac{\alpha_s}{2\pi} x \bar{P}_{gg}(x) \left[-\frac{1}{\epsilon} - \ln \left(\frac{\bar{\mu}^2 x \bar{N}}{M^2} \right) \right] + \frac{\alpha_s}{2\pi} x(1-x) P_{gg}(x) \left(\frac{\ln(1-x)}{1-x} \right)_+ .
\end{aligned}$$

This expression for the partonic QCD cross section is needed for the matching calculations in the next section.

IV. MATCHING

In this section, we match QCD onto SCET_I at the scale $\bar{\mu} = M$ and then SCET_I onto SCET_{II} at the scale $\bar{\mu} = M/\sqrt{N}$. At the first stage we must verify that SCET_I reproduces the IR behavior of QCD, i.e. the SCET_I real emission diagrams must reproduce the terms in Eq. (46) which dominate as $z \rightarrow 1$. At the second stage of matching, the SCET_I cross section is matched on the SCET_{II} cross section, which takes on the factorized form of Eq. (27). These calculations are simplest if dimensional regularization is used to regulate both ultraviolet (UV) and IR divergences. The matching calculations are important for verifying the factorization theorem and determining the QCD-SCET_I and SCET_I-SCET_{II} matching scales, which give the boundary conditions for renormalization group evolution.

A. Matching QCD onto SCET_I

In the first step we match the QCD amplitude onto the SCET_I current at one loop. The one-loop QCD result for the virtual correction can be found in Ref. [32],

$$\begin{aligned} \frac{d\hat{\sigma}}{dz} &= (\sigma_0 + \sigma^{(V)})\delta(1-x)\delta(1-z), \\ \sigma^{(V)} &= \sigma_0 \frac{\alpha_s}{2\pi} f_\epsilon(M^2) \left\{ \frac{b_0}{\epsilon_{\text{UV}}} + \left(C_F - \frac{1}{2}C_A \right) \frac{\pi^2}{v} - C_A \left(\frac{1}{\epsilon_{\text{IR}}^2} + \frac{17}{6\epsilon_{\text{IR}}} \right) + \frac{2}{3\epsilon_{\text{IR}}} n_f T_F + 2D_{\mathcal{O}}^{[8]} \right\}, \end{aligned} \quad (52)$$

where $C_F = 4/3$, $C_A = 3$, $T_F = 1/2$ are SU(3) group theory factors, n_f is the number of light flavors, v is the relative velocity of the c and \bar{c} in the rest frame of the $c\bar{c}$ pair, and

$$\begin{aligned} f_\epsilon(M^2) &= \left(\frac{4\pi\mu^2}{M^2} \right)^\epsilon \Gamma(1+\epsilon), \\ D_{1S_0}^{[8]} &= C_F \left(-5 + \frac{\pi^2}{4} \right) + C_A \left(\frac{3}{2} + \frac{\pi^2}{12} \right), \\ D_{3P_0}^{[8]} &= C_F \left(-\frac{7}{3} + \frac{\pi^2}{4} \right) + C_A \left(\frac{1}{2} + \frac{\pi^2}{12} \right), \\ D_{3P_2}^{[8]} &= -4C_F + C_A \left(\frac{3}{4} + \frac{\log 2}{2} + \frac{\pi^2}{3} \right). \end{aligned} \quad (53)$$

The UV divergence in Eq. (52) is removed by QCD coupling constant renormalization. When computing the matching coefficient to this order, one must include one-loop NRQCD virtual corrections to the matrix element of the NRQCD color-octet production operators. The NRQCD corrections reproduce the Coulomb correction $\propto \pi^2/v$ in Eq. (52) and therefore this term does not appear in the matching coefficient [33].

In SCET_I loop integrals are scaleless in dimensional regularization and therefore are zero. We must also subtract the contribution from the EFT counterterm which was calculated in Ref. [34]:

$$Z_{\mathcal{O}} - 1 = \frac{\alpha_s}{4\pi} \left[C_A \left(\frac{1}{\epsilon^2} + \frac{1}{\epsilon} \log \left(\frac{\bar{\mu}^2}{M^2} \right) + \frac{17}{6\epsilon} \right) - \frac{2}{3\epsilon} n_f T_F \right]. \quad (54)$$

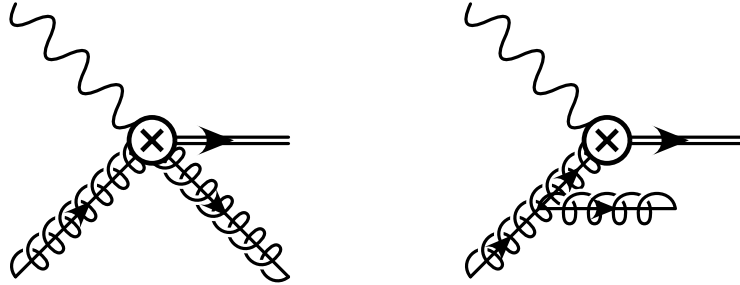


FIG. 3: *Feynman graphs for the real emission of a collinear gluon.*

Thus the SCET_I one loop result for the virtual cross section is

$$\frac{d\hat{\sigma}}{dz} = \sigma_0 |C_V(\bar{\mu})|^2 \delta(1-z) \left(1 + \frac{\alpha_s}{2\pi} \left\{ -C_A \left[\frac{1}{\epsilon^2} + \frac{1}{\epsilon} \log \left(\frac{\bar{\mu}^2}{M^2} \right) + \frac{17}{6} \right] + \frac{2}{3\epsilon} n_f T_F \right\} \right). \quad (55)$$

Taking the difference between this and Eq. (52) (after subtracting the UV divergence and dropping the Coulomb correction) we obtain the one loop matching coefficient

$$C_V(\bar{\mu}) = 1 + \frac{\alpha_s}{4\pi} \left[-C_A \left(\frac{1}{2} \log^2 \frac{\bar{\mu}^2}{M^2} + \frac{17}{6} \log \frac{\bar{\mu}^2}{M^2} + \frac{\pi^2}{12} \right) + \frac{2}{3} n_f T_F \log \frac{\bar{\mu}^2}{M^2} + 2D_{\mathcal{O}}^{[8]} \right]. \quad (56)$$

The logarithms are minimized for $\bar{\mu} = M$, which fixes the QCD-SCET_I matching scale.

B. The NLO SCET_I differential cross section and matching onto SCET_{II}

In the second step we match the SCET_I differential cross section onto the SCET_{II} differential cross section which has the factored form given in Eq. (27). The calculation of the SCET_I differential cross section at NLO also allows us to confirm that the EFT reproduces the parts of the NLO QCD calculation that are singular as $z \rightarrow 1$. This is an important check on the validity of the EFT.

The SCET diagrams for the real emission come from both collinear and usoft graphs. These are shown in Figs. (3) and (4), respectively. The result of the usoft graphs is the same as making the eikonal approximation in the full QCD diagram [32]:

$$\frac{d\hat{\sigma}^{\text{soft}}}{dz} = \sigma_0 \frac{C_A \alpha_s}{\pi} \frac{x^\epsilon (1-z)^{-\epsilon} (z-x)^{-\epsilon}}{\Gamma[1-\epsilon]} \left[\frac{x^2}{(1-z)(1-x)} - \frac{x^2}{(1-x)^2} \right]. \quad (57)$$

Evaluation of the collinear graphs is more subtle. A naive evaluation employing the Feynman rules of Ref. [21] yields

$$\frac{d\hat{\sigma}^{\text{col}}}{dz} = \sigma_0 \frac{C_A \alpha_s}{\pi} \frac{x^\epsilon (1-z)^{-\epsilon} (z-x)^{-\epsilon}}{\Gamma[1-\epsilon]} \left[\frac{x^2 (1+x-z+(x-z)^2)^2}{(1-z)(z-x)(1+x-z)^2} \right]. \quad (58)$$

Note that the naive collinear contribution to the cross section has pole in $z-x$ that is not present in the full QCD calculation in Eq. (43). Combining the cross sections in Eq. (57)

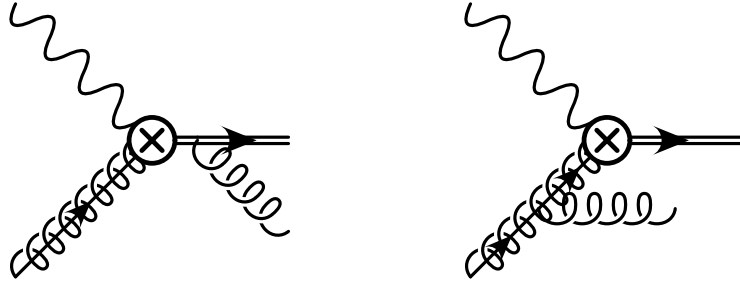


FIG. 4: Feynman graphs for the real emission of a usoft gluon.

and Eq. (58) then expanding about $z = 1$ as was done earlier for $\mathcal{M}(x, z)$ does not yield the two leading terms in Eq. (46).

The origin of this problem is double counting of modes in certain corners of phase space where modes can be considered either collinear or usoft [27]. Collinear particles in SCET have momentum scaling as $Q(\lambda^2, 1, \lambda)$. For the bulk of the phase space integration, this scaling is satisfied but when $x, z \rightarrow 1$ simultaneously it is not. To see this note that the momentum of the final state gluon in the real emission diagrams is

$$\begin{aligned} k^\mu &= \frac{1}{2}\sqrt{\hat{s}}(1-z)\bar{n}^\mu - \frac{1}{2}\sqrt{\hat{s}}(x-z)n^\mu + k_\perp^\mu, \\ k_\perp^2 &= -\hat{s}(x-z)(1-z). \end{aligned} \quad (59)$$

For $1-z \sim O(\lambda^2)$ and $x-z \sim O(1)$ we see that the final state gluon momentum scales as

$$(n \cdot k, \bar{n} \cdot k, k_\perp) \sim \sqrt{\hat{s}}(\lambda^2, 1, \lambda),$$

appropriate for a collinear particle. However, the phase space integral over x ranges from (nearly) zero to z , so there is a corner of phase space in which $x-z \sim O(\lambda^2)$ rather than $O(1)$ and therefore

$$(n \cdot k, \bar{n} \cdot k, k_\perp) \sim \sqrt{\hat{s}}(\lambda^2, \lambda^2, \lambda^2).$$

In this regime the scaling is appropriate for a usoft particle.

In the SCET label formalism, double counting arises from a naive evaluation of the sums over collinear label momenta appearing in loops and phase space integrations. The mode with vanishing label momentum, the so-called “zero-bin”, must be excluded from these sums since a mode with vanishing collinear label momentum should be considered soft. As discussed in Appendix B, the standard trick for converting sums over label momenta with integrations over residual momenta to obtain ordinary loop and phase space integrals actually includes the zero-bin mode, and therefore certain zero-bin subtractions must be made to correctly evaluate collinear diagrams.

In our problem, the zero-bin subtraction can be implemented by including additional diagrams that are identical to the collinear diagrams except that the momentum of the final state gluon is treated as usoft and the appropriate approximations are made. This graph gives

$$\frac{d\sigma^{\text{zb}}}{dz} = \sigma_0 \frac{C_A \alpha_s}{\pi} \frac{x^\epsilon (1-z)^{-\epsilon} (z-x)^{-\epsilon}}{\Gamma[1-\epsilon]} \left[\frac{-x^2}{(1-z)(z-x)} \right]. \quad (60)$$

The minus sign reflects the fact that we must subtract the zero-bin contribution from the naive evaluation of the collinear contribution. Combining the usoft, collinear, and zero-bin subtraction yields

$$\begin{aligned} \frac{d\sigma}{dz} &= \sigma_0 \frac{C_A \alpha_s}{\pi} \frac{x^\epsilon (1-z)^{-\epsilon} (z-x)^{-\epsilon}}{\Gamma[1-\epsilon]} \times \\ &\left[\frac{x^2}{(1-z)(z-x)} \left(\frac{(1+x-z+(x-z)^2)^2}{(1+x-z)^2} - 1 \right) + \frac{x^2}{(1-z)(1-x)} - \frac{x^2}{(1-x)^2} \right] \\ &= \sigma_0 \frac{C_A \alpha_s}{\pi} \frac{x^\epsilon (1-z)^{-\epsilon} (z-x)^{-\epsilon}}{\Gamma[1-\epsilon]} \left[\frac{(1+x-x^2)^2}{(1-z)(1-x)} - \frac{1}{(1-x)^2} + \dots \right], \end{aligned} \quad (61)$$

where the ellipsis represents terms which do not contribute logarithmically enhanced corrections. We see that once the zero-bin contribution is subtracted, the spurious pole at $x = z$ is removed and the leading behavior of the QCD cross section is reproduced by SCET_I, as expected.

To get the SCET_I differential cross section to this order we must add the virtual contributions. Loops are scaleless and therefore vanish in dimensional regularization, but the contribution from tree level graphs with the counterterm in Eq. (54) must also be included. We will match the moments of the partonic cross sections rather than the partonic differential cross sections. Combining the SCET_I real emission contribution with the SCET_I counterterm contribution, we obtain

$$\begin{aligned} \frac{\hat{\sigma}_N^I}{\sigma_0} &= -\frac{\alpha_s}{2\pi} x \mathcal{P}_{gg}(x) \frac{1}{\epsilon} \\ &+ \delta(1-x) \frac{C_A \alpha_s}{\pi} \left[\frac{1}{4} \ln^2 \left(\frac{\bar{\mu}^2}{M^2} \right) + \frac{1}{2} \ln \left(\frac{\bar{\mu}^2}{M^2} \right) + \ln(\bar{N}) - \frac{1}{2} \ln^2(\bar{N}) - \frac{\pi^2}{8} \right] \\ &- \frac{\alpha_s}{2\pi} x \bar{\mathcal{P}}_{gg}(x) \ln \left(\frac{\bar{\mu}^2 x \bar{N}}{M^2} \right) + \frac{\alpha_s}{2\pi} x(1-x) P_{gg}(x) \left(\frac{\ln(1-x)}{1-x} \right)_+. \end{aligned} \quad (62)$$

In SCET_{II}, the partonic cross section takes on the factorized form of Eq. (34), except now the initial state is a gluon rather than a nucleon:

$$\frac{\hat{\sigma}_N^{II}}{\sigma_0} = x \tilde{S}^{(8,1s_0)}(N) \int_x^1 \frac{d\xi}{\xi} \hat{C}_{II} \left(\frac{x}{\xi}, N \right) f_{g/g}(\xi). \quad (63)$$

In Eq. (63), we need the one loop result for the moments of the shape function,

$$S^{(8,1s_0)}(N) = 1 - \frac{\alpha_s C_A}{\pi} \left[\log^2 \left(\frac{\bar{\mu} \bar{N}}{M} \right) - \log \left(\frac{\bar{\mu} \bar{N}}{M} \right) \right], \quad (64)$$

and the one loop expression for the gluon structure function [35]

$$f_{g/g}(\xi) = \delta(1-\xi) - \frac{1}{\epsilon} \frac{\alpha_s}{2\pi} \mathcal{P}_{gg}(\xi). \quad (65)$$

Parametrizing the matching coefficient \hat{C}_{II} as

$$\frac{x}{\xi} \hat{C}_{II} \left(\frac{x}{\xi}, N \right) = \delta \left(1 - \frac{x}{\xi} \right) \left(1 + \alpha_s \hat{C}_{II}^{(1)}(N) \right) + \alpha_s \hat{C}_{II}^{(2)} \left(\frac{x}{\xi}, N \right), \quad (66)$$

inserting into Eq. (63) and expanding to $O(\alpha_s)$ we find

$$\begin{aligned} \frac{\hat{\sigma}_N^{II}}{\sigma_0} = & \delta(1-x) \left[1 + \alpha_s \hat{C}_{II}^{(1)}(N) - \frac{\alpha_s C_A}{\pi} \left[\log^2 \left(\frac{\bar{\mu} \bar{N}}{M} \right) - \log \left(\frac{\bar{\mu} \bar{N}}{M} \right) \right] \right] \\ & - \frac{1}{\epsilon} \frac{\alpha_s}{2\pi} x \mathcal{P}_{gg}(x) + \alpha_s \hat{C}_{II}^{(2)}(x, N). \end{aligned} \quad (67)$$

Comparing Eq. (62) and Eq. (67) we obtain the matching coefficient C_{II} to $O(\alpha_s)$:

$$\begin{aligned} \hat{C}_{II}(x, N) = & \delta(1-x) \left(1 + \frac{C_A \alpha_s}{\pi} \left[\frac{1}{2} \ln^2 \left(\frac{\bar{\mu}^2 \bar{N}}{M^2} \right) - \frac{\pi^2}{8} \right] \right) \\ & - \frac{\alpha_s}{2\pi} \bar{P}_{gg}(x) \ln \left(\frac{\bar{\mu}^2 x \bar{N}}{M^2} \right) + \frac{\alpha_s}{2\pi} (1-x) P_{gg}(x) \left(\frac{\ln(1-x)}{1-x} \right)_+. \end{aligned} \quad (68)$$

This result shows that all large logs of N in the matching coefficient vanish at the intermediate scale $\bar{\mu} = M/\sqrt{\bar{N}}$, which fixes the SCET_I-SCET_{II} matching scale. At this scale there remains a $\ln(x)$ in the matching coefficient which is $O(1)$ in our power counting.

V. RUNNING

In this section the renormalization group is used to resum large logs of N in the moments of the cross section. An inverse Mellin transform of the resummed moments is performed to obtain an analytic resummed formula for the differential cross section. The evolution is carried out in two stages. First, we run the effective theory currents in Eq. (6) using the SCET_I RGEs from the scale $\bar{\mu} = M$, where QCD is matched onto SCET_I, to the scale $\bar{\mu} = M/\sqrt{\bar{N}}$, where SCET_I is matched onto SCET_{II}. Second, the shape function in SCET_{II} is run down to the scale $\bar{\mu} = M/\bar{N}$.

The currents that arise in photoproduction also arise in radiative decays, and the running was calculated in Ref. [34]:

$$\begin{aligned} \log \left[\frac{C_V(\mu)}{C_V(M)} \right] = & - \frac{4\pi \Gamma_1^{\text{adj}}}{\beta_0^2 \alpha_s(M)} \left[\frac{1}{y} - 1 + \log y \right] - \frac{\Gamma_1^{\text{adj}} \beta_1}{\beta_0^3} \left[1 - y + y \log y - \frac{1}{2} \log^2 y \right] \\ & - \frac{B_1 + 2\gamma_1}{\beta_0} \log y - \frac{4\Gamma_2^{\text{adj}}}{\beta_0^2} \left[y - 1 - \log y \right], \end{aligned} \quad (69)$$

where $y = \alpha_s(\mu)/\alpha_s(M)$ and

$$\begin{aligned} \Gamma_1^{\text{adj}} &= C_A, \quad \Gamma_2^{\text{adj}} = C_A \left[C_A \left(\frac{67}{36} - \frac{\pi^2}{12} \right) - \frac{5n_f}{18} \right], \\ B_1 &= -C_A, \quad \gamma_1 = -\frac{\beta_0}{4}, \quad \beta_0 = \frac{11}{3} C_A - \frac{2}{3} n_f. \end{aligned} \quad (70)$$

The two loop cusp anomalous dimension Γ_2^{adj} was first calculated in Refs. [36, 37]. At leading order $C_V(M) = 1$.

In the second stage, only the shape function is evolved. This is possible since the soft and collinear sectors in SCET_{II} are decoupled. Denoting the scales in the collinear and soft

sectors as $\bar{\mu}_c$ and $\bar{\mu}_s$ respectively, and making the scales explicit in Eq. (30), we have

$$\begin{aligned} \frac{d\sigma}{dz} &= \rho \sigma_0 C_V^2(\bar{\mu}_c) \int dk^+ S^{(8,1S_0)}(\sqrt{s}(1-z) - k^+; \bar{\mu}_s) \\ &\times \int_\rho^1 \frac{d\xi}{\xi} C_{II}\left(\frac{\rho}{\xi}, k^+; \bar{\mu}_c\right) f_{g/P}(\xi; \bar{\mu}_c). \end{aligned} \quad (71)$$

In this section, we focus on the $^1S_0^{(8)}$ contribution to the cross section. The expression for the resummed cross section is easily generalized to $^3P_J^{(8)}$ channels since the evolution equations are identical. In matching SCET_I onto SCET_{II} we must set $\bar{\mu}_s = \bar{\mu}_c = M/\sqrt{N}$ in order to minimize logarithms in the matching coefficient C_{II} . However, the shape function will still contain large logarithms of N . The shape function must be evolved from $\bar{\mu}_s = M/\sqrt{N}$ to $\bar{\mu}_s = M/\bar{N}$ to minimize its logarithms.

The running of the soft function is easily carried out in moment space where the differential cross section is a product of the moments of the shape function and moments of the hard coefficient, as in Eq. (34),

$$\sigma_N = \rho \sigma_0 C_V^2(\bar{\mu}_c) \tilde{S}^{(8,1S_0)}(N; \bar{\mu}_s) \int_\rho^1 \frac{d\xi}{\xi} \hat{C}_{II}\left(\frac{\rho}{\xi}, N; \bar{\mu}_c\right) f_{g/P}(\xi; \bar{\mu}_c). \quad (72)$$

The anomalous dimension of the shape function can be calculated by replacing the J/ψ projection operator $\mathcal{P}_\psi = a_\psi^\dagger a_\psi$ with an on-shell charm projection operator $\mathcal{P}_{c\bar{c}}$ since the renormalization of an operator is only sensitive to short distances. The tree and one gluon Feynman rules are the same Feynman rules as those of the shape function that appears in quarkonium decay, and the one loop calculation of the shape function in Ref. [34] gives

$$\gamma(N; \bar{\mu}) = \frac{\alpha_s(\bar{\mu}) C_A}{\pi} \left[1 - 2 \log\left(\frac{\bar{\mu}\bar{N}}{M}\right) \right]. \quad (73)$$

The RGE can be solved in moment space. Combining the running in SCET_I of the currents in Eq. (69) with the evolution of the shape function, we obtain the following resummed expression for the moments of the J/ψ photoproduction cross section:

$$\begin{aligned} \sigma_N &= \rho \sigma_0 e^{\log(N)g_1(\chi) + g_2(\chi)} \tilde{S}^{(8,1S_0)}(N; M/\bar{N}) \\ &\times \int_\rho^1 \frac{d\xi}{\xi} \hat{C}_{II}\left(\frac{\rho}{\xi}, N; M/\sqrt{\bar{N}}\right) f_{g/P}(\xi; M/\sqrt{\bar{N}}), \end{aligned} \quad (74)$$

where

$$\begin{aligned} g_1(\chi) &= -\frac{2\Gamma_1^{\text{adj}}}{\beta_0\chi} [(1-2\chi)\log(1-2\chi) - 2(1-\chi)\log(1-\chi)], \\ g_2(\chi) &= -\frac{8\Gamma_2^{\text{adj}}}{\beta_0^2} [-\log(1-2\chi) + 2\log(1-\chi)] \\ &\quad -\frac{2\Gamma_1^{\text{adj}}\beta_1}{\beta_0^3} \left[\log(1-2\chi) - 2\log(1-\chi) + \frac{1}{2}\log^2(1-2\chi) - \log^2(1-\chi) \right] \\ &\quad + \frac{4\gamma_1}{\beta_0} \log(1-\chi) + \frac{2B_1}{\beta_0} \log(1-2\chi) \\ &\quad - \frac{4\Gamma_1^{\text{adj}}}{\beta_0} \log n_0 [\log(1-2\chi) - \log(1-\chi)], \end{aligned} \quad (75)$$

with $n_0 = e^{\gamma_E}$, $\chi = \log(N) \alpha_s(M) \beta_0 / 4\pi$, and $\beta_1 = (34C_A^2 - 10C_A n_f - 6C_F n_f) / 3$.

To obtain the resummed expression for the differential cross section, $d\sigma/dz$, we take the inverse Mellin transform of the expression in Eq. (74). However, this is complicated since the scale in the pdf depends on N . To perform the inverse Mellin transform we must first undo the convolution in Eq. (74) by taking moments with respect to ρ :

$$\begin{aligned} \frac{\tilde{\sigma}_N(K)}{\sigma_0} &= \frac{1}{\sigma_0} \int_0^1 d\rho \rho^{K-1} \sigma_N(\rho) \\ &= e^{\log(N)g_1(\chi)+g_2(\chi)} \tilde{S}^{(8,1S_0)}(N; M/\bar{N}) \\ &\quad \times \int_0^1 d\rho \rho^K \int_\rho^1 \frac{d\xi}{\xi} \hat{C}_{II} \left(\frac{\rho}{\xi}, N; M/\sqrt{\bar{N}} \right) f_{g/P}(\xi; M/\sqrt{\bar{N}}) \\ &= e^{\log(N)g_1(\chi)+g_2(\chi)} \tilde{S}^{(8,1S_0)}(N; M/\bar{N}) \tilde{C}_{II} \left(K, N; M/\sqrt{\bar{N}} \right) \tilde{f}_{g/P}(K; M/\sqrt{\bar{N}}), \end{aligned} \quad (76)$$

where

$$\begin{aligned} \tilde{C}_{II}(K, N; \mu) &= \int_0^1 d\xi \xi^K \hat{C}_{II}(\xi, N; \mu), \\ \tilde{f}_{g/P}(K; \mu) &= \int_0^1 d\xi \xi^K f_{g/P}(\xi; \mu). \end{aligned} \quad (77)$$

The dependence of the pdf on the scale $M/\sqrt{\bar{N}}$ can be made explicit by using the evolution equations for the moments of the structure function. Ignoring mixing, the running of the pdf in moment space is given by

$$\mu \frac{d}{d\mu} \tilde{f}_{g/P}(K; \mu) = \frac{\alpha_s(\mu)}{4\pi} a_{gg}(K) \tilde{f}_{g/P}(K; \mu), \quad (78)$$

where the explicit form of $a_{gg}(K)$ is not needed in what follows. The leading order solution of Eq. (78) in moment space is

$$\tilde{f}_{g/P} \left(K; M/\sqrt{\bar{N}} \right) = \tilde{f}_{g/P}(K; M) \exp \left[\frac{a_{gg}(K)}{2\beta_0} \log(1 - \chi) \right] \equiv \tilde{f}_{g/P}(K; M) \exp [h_K(\chi)]. \quad (79)$$

The pdf on the right hand side of this equation is evaluated at the scale M , and is therefore independent of N . All N dependence has been moved into the factor $h_K(\chi)$. Using this result in Eq.(76) we get

$$\frac{\tilde{\sigma}_N(K)}{\sigma_0} = e^{\log(N)g_1(\chi)+g_2(\chi)+h_K(\chi)} \tilde{S}^{(8,1S_0)}(N; M/\bar{N}) \tilde{C}_{II}(K, N; M/\sqrt{\bar{N}}) \tilde{f}_{g/P}(K; M). \quad (80)$$

Since the logarithms in $\hat{C}_{II}(x, N)$ are minimized at the scale $M/\sqrt{\bar{N}}$, $\tilde{C}_{II}(K, N; M/\sqrt{\bar{N}}) = 1 + O(\alpha_s)$, where the $O(\alpha_s)$ term has no logarithmically enhanced contributions. Therefore, we can set $\tilde{C}_{II}(K, N; M/\sqrt{\bar{N}}) = 1$, making it possible to analytically evaluate the inverse Mellin transforms with respect to both N and K . Using the results of Ref. [38] to evaluate the inverse Mellin transform with respect N yields

$$\begin{aligned} \frac{d\tilde{\sigma}(z, K)}{dz} &= \sigma_0 \int_z^1 \frac{du}{u} \hat{S}^{(8,1S_0)}(z/u) \\ &\quad \times \left(-u \frac{d}{du} \left\{ \Theta(1-u) \frac{e^{lg_1(l)+g_2(l)+h_K(l)}}{\Gamma[1-g_1(l)-lg_1'(l)]} \right\} \right) \tilde{f}_{g/P}(K; M), \end{aligned} \quad (81)$$

where $l = -\alpha_s \beta_0 / (4\pi) \log(1 - u)$ and $g_1'(l) = dg_1(l)/dl$. Next, we eliminate the factor $h_K(l)$ using the leading order solution of Eq. (78) again,

$$e^{h_K(l)} \tilde{f}_{g/P}(K; M) = \tilde{f}_{g/P}(K; M) \exp \left[\frac{a_{gg}(K)}{2\beta_0} \log(1 - l) \right] = \tilde{f}_{g/P}(K; M\sqrt{1 - u}). \quad (82)$$

Using this result in Eq. (81) we arrive at

$$\begin{aligned} \frac{d\tilde{\sigma}(z, K)}{dz} &= \sigma_0 \int_z^1 \frac{du}{u} \hat{S}^{(8,1S_0)}(z/u) \\ &\times \left(-u \frac{d}{du} \left\{ \Theta(1 - u) \frac{e^{lg_1(l)+g_2(l)}}{\Gamma[1 - g_1(l) - lg_1'(l)]} \tilde{f}_{g/P}(K; M\sqrt{1 - u}) \right\} \right). \end{aligned} \quad (83)$$

The K dependence is now entirely contained in the moments of the pdf, so the inverse Mellin transform with respect to K is trivial. The fully resummed differential cross section is

$$\begin{aligned} \frac{d\sigma}{dz} &= \rho \sigma_0 \int_z^1 \frac{du}{u} \hat{S}^{(8,1S_0)}(z/u) \\ &\times \left(-u \frac{d}{du} \left\{ \Theta(1 - u) \frac{e^{lg_1(l)+g_2(l)}}{\Gamma[1 - g_1(l) - lg_1'(l)]} f_{g/P}(\rho; M\sqrt{1 - u}) \right\} \right). \end{aligned} \quad (84)$$

This result is unusual because the scale of the pdf varies between $M\sqrt{1 - z} \sim \sqrt{M\Lambda_{QCD}}$ and 0 in the convolution integral. It is not clear how to evaluate the pdf when the scale is below Λ_{QCD} . Another problem arises in the resummed coefficient since the functions $g_i(l)$ blow up for u sufficiently close to 1. If the resummed exponent is expressed as an integral over a running coupling this divergence is due to the Landau pole. This problem commonly arises in resummed calculations and a prescription for dealing with the Landau pole is required for phenomenological work. In what follows we cut off the integral at an upper limit, $u_{max} = 0.93$, which is set by the location of the Landau pole. For this value of u_{max} the lowest scale at which the pdf needs to be evaluated is 800 MeV, so the prescription for dealing with the Landau pole in the resummed exponent also fixes the problem associated with the scale of the pdf. The difference between integrating to u_{max} as opposed to one is formally the same order as power suppressed corrections and therefore can be systematically neglected [39]. Likewise, the difference between the prescription used in this paper and other possible prescriptions is of order power suppressed corrections. An alternative approach which explicitly avoids the Landau pole is given in Ref. [40].

VI. PHENOMENOLOGY

Before we can investigate the phenomenological consequences of our resummed cross section, we must determine the shape functions. Unfortunately not much is known about these nonperturbative functions, although they also arise in $e^+ + e^- \rightarrow J/\psi + X$ and electroproduction [19]. A fit of the shape function to Belle [41] and Babar [42] data on $e^+ + e^- \rightarrow J/\psi + X$ was carried out in Ref. [21], and we will use the parameters determined from that fit in our calculation. We use these shape functions for illustrative purposes only, as the shape functions extracted in Ref. [21] are not reliable. The Belle collaboration observes that the J/ψ cross section at $\sqrt{s} = 10.6$ GeV is dominated by events with an

additional $c\bar{c}$ pair, i.e., $e^+ + e^- \rightarrow J/\psi + c + \bar{c} + X$ [43, 44]. This fact is poorly understood at the present time [45] and we do not expect the color-octet mechanism studied in this paper to contribute significantly to $e^+ + e^- \rightarrow J/\psi + c + \bar{c} + X$. A sensible extraction of the color-octet shape function from $e^+ + e^- \rightarrow J/\psi + X$ requires removal of events with extra $c\bar{c}$ pairs, and such data is not currently available.

For simplicity, we assume that the $^1S_0^{(8)}$ and $^3P_J^{(8)}$ shape functions are the same, but this need not be the case. The shape function model we adopt is a modified version of a model used in the decay of B mesons [46],

$$f(r^+) = \frac{1}{\bar{\Lambda}} \frac{a^{ab}}{\Gamma(ab)} (x-1)^{ab-1} e^{-a(x-1)} \theta(x-1), \quad x = \frac{r^+}{\bar{\Lambda}}, \quad (85)$$

where a and b are adjustable parameters and $\bar{\Lambda} = M_\psi - M$. This function is related to the shape function *only* in the J/ψ rest frame where $f(-r^+) = S(r^+)$. To relate the model above to the shape function $\hat{S}(u)$ which appears in Eq. (84) we use boost invariance

$$dk^+ S(-\sqrt{s}(1-z) + k^+) \rightarrow dl^+ S(-M(1-z) + l^+), \quad (86)$$

where $l^+ = (M/\sqrt{s})k^+$ is the rest frame residual momentum which is $O(\Lambda_{\text{QCD}})$. Since $dk^+ = (\sqrt{s}/M)dl^+$ we get $S(-\sqrt{s}(1-z) + k^+) \rightarrow (M/\sqrt{s})S(-M(1-z) + l^+)$. Finally we get

$$\begin{aligned} \hat{S}(z-u) &= \sqrt{s} S(-\sqrt{s}(1-z) + k^+) \\ &\rightarrow MS(-M(1-z) + l^+) \\ &= Mf(M(1-z) - l^+) = Mf(M(u-z)), \end{aligned} \quad (87)$$

where in the J/ψ rest frame $l^+ \equiv M(1-u)$.

The first three moments $f(r^+)$ are

$$\begin{aligned} m_0 &= \int_{\bar{\Lambda}}^{\infty} dr^+ f(r^+) = 1, & m_1 &= \int_{\bar{\Lambda}}^{\infty} dr^+ r^+ f(r^+) = \bar{\Lambda}(b+1), \\ m_2 &= \int_{\bar{\Lambda}}^{\infty} dr^+ (r^+)^2 f(r^+) = \bar{\Lambda}^2 \left(\frac{b}{a} + (b+1)^2 \right). \end{aligned} \quad (88)$$

Since $\bar{\Lambda} \sim \mathcal{O}(\Lambda_{\text{QCD}})$, any choice with $a \sim b \sim \mathcal{O}(1)$ gives the desired scaling for the moments. We use parameters taken from a fit to the $e^+ + e^- \rightarrow J/\psi + X$ data [21]: $a = 1, b = 2$. The value of the first and second moments of the shape function for this choice of parameters are 890 MeV and $(985 \text{ MeV})^2$ respectively. Since $m_c v^2 \approx 500 \text{ MeV}$ the moments are consistent with the velocity scaling rules.

Calculations of $d\sigma/dz$ are shown in Fig. 5. The solid line is the final result, Eq. (84), normalized to σ_0 using the shape function in Eq. (85). The dashed line is a plot of the shape function alone and the dotted line includes only the perturbative resummation. Here we use $m_c = 1.4 \text{ GeV}$, $\sqrt{s} = 100 \text{ GeV}$, and the CTEQ5L pdfs [47]. Fig. 5 shows the effects of both the perturbative resummation and the shape function. The results are very similar to other resummed calculations: the perturbative resummation alone or the shape function alone give a cross section that is highly peaked in the endpoint region. In contrast, the convoluted result is much broader with the peak shifted to lower values of z .

It is important to point out that the calculation is not valid for z very close to one. Though SCET is valid in the endpoint region, the calculation assumes that the final state

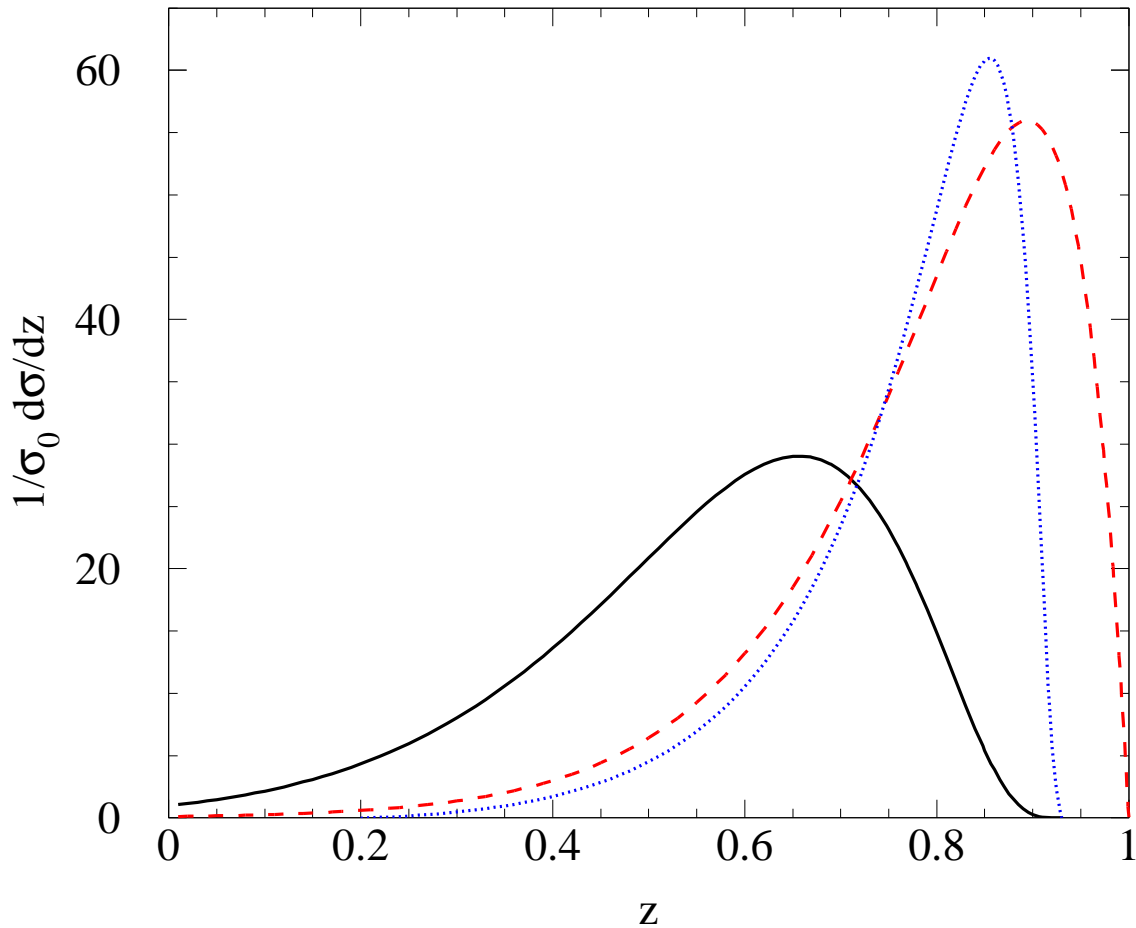


FIG. 5: *The color-octet contribution at the endpoint normalized to σ_0 . The solid line is the perturbative resummation convoluted with the shape function. The dotted line is perturbative resummation only, and the dashed line is no resummation, but including a shape function.*

is inclusive. However, as z gets very close to one the cross section is dominated by exclusive final states. This occurs when $M(1-z) \sim \Lambda_{\text{QCD}}$, which is roughly $z \sim 0.9$. In this exclusive region our analysis is not valid and a very different approach is needed.

In Fig. 6 we show the differential cross section. The short dashed line is the color-octet contribution, which has a normalization set by the linear combination of color-octet matrix elements in Eq. (41). We set this combination to $3 \cdot 10^{-3}$, which is an order of magnitude smaller than the value determined from a fit to Tevatron data. The long dashed curve is the color-singlet contribution, and the solid curve is the sum of singlet and octet. The singlet contribution is peaked in the endpoint and it is not possible to compare to data until a

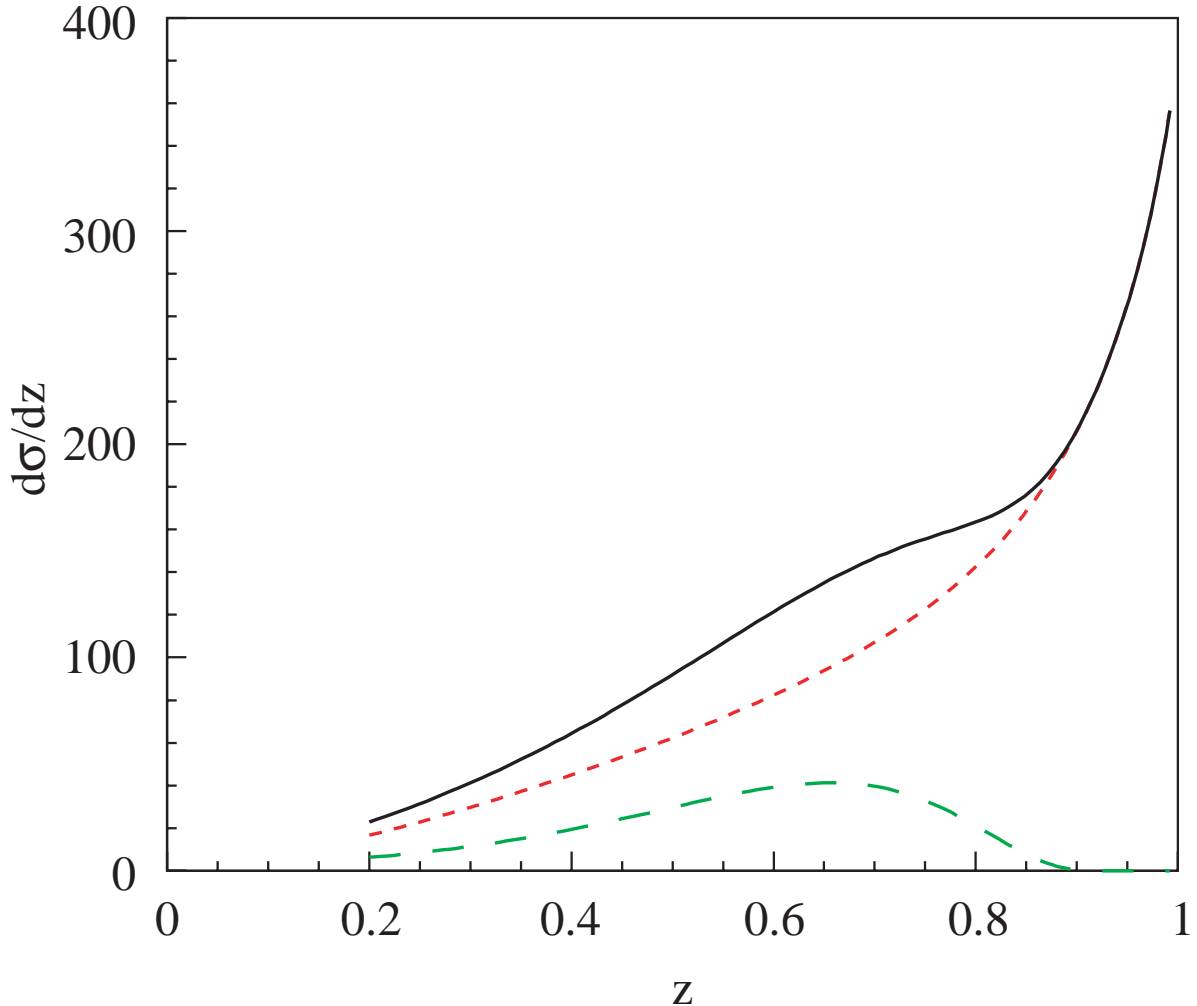


FIG. 6: *The differential cross section in nb. The resummed color-octet contribution (short dashes), the leading order color-singlet contribution (long dashes), and the sum (solid line). The rise in the differential cross section at the endpoint due to the color-singlet contribution must be resummed before a meaningful comparison to data can be made.*

resummation of the singlet contribution is completed. This work is in progress [48].

The analysis of Ref. [9] indicates that the data is well described by the color-singlet cross section alone so it appears that there is little room for a color-octet contribution. A naive fit with the leading-order color-singlet calculation and the resummed color-octet cross section would lead to the conclusion that color-octet matrix elements are smaller than those obtained from fitting to Tevatron data. However there are caveats. First, large endpoint effects in color-singlet production also need to be resummed. While we do not expect the results of this resummation to be as dramatic as in color-octet production, resummation should also suppress color-singlet production in the endpoint region, creating more room for a color-octet contribution to photoproduction. Second, most of the available data has cuts that remove any contribution for $p_{\perp} < 1$ GeV. In our calculation we integrated over p_{\perp} assuming $p_{\perp} < M$. Thus care must be taken when comparing to experimental measurements.

The Zeus collaboration has carried out an analysis which includes a measurement of $d\sigma/dz$ with no p_\perp cut as well as a cut of 1 GeV and 2 GeV [49]. The data clearly show that a p_\perp cut decreases the differential cross section with the greatest reduction being in the high z bins. Thus comparing to data with no p_\perp cut may allow for a larger color-octet contribution. Furthermore it is common practice to cut out the diffractive contribution from the data. However, our calculation assumes that the diffractive contribution is part of the complete sum over final states, and an honest comparison requires data without the diffractive contribution subtracted. The Zeus analysis of Ref. [49] gives the percentage by which the cross section decreases when the diffractive contribution is removed. Again this fraction becomes large as the endpoint region is approached, and including the diffractive contribution in the experimental measurement could lead to greater room for a color-octet contribution.

VII. SUMMARY

In this paper we studied the color-octet contribution to J/ψ photoproduction near the kinematic endpoint. As $z \rightarrow 1$ the usual NRQCD factorization formalism breaks down due to large perturbative and nonperturbative corrections. We combined SCET with NRQCD to derive a factorization theorem for the differential cross section, $d\sigma/dz$, in the endpoint region in terms of the parton distribution function and nonperturbative color-octet shape functions. Large Sudakov logarithms which appear in the endpoint are resummed using the RGE of the effective theory.

Since the total photoproduction cross section is largely accounted for by the color-singlet term in NRQCD a resummation of this contribution must be carried out before a quantitative comparison to data can be made. However, some qualitative conclusions can be drawn. First, we find that perturbative resummation acts constructively with the shape function to significantly broaden the z distribution. This important effect improves the agreement between the shape of the theoretical prediction and data. Second, the normalization of our prediction is set by a linear combination of NRQCD matrix elements which also appear in calculations of J/ψ production at the Tevatron. The data clearly prefer values for the color-octet matrix elements that are roughly an order of magnitude smaller than the central values extracted from Tevatron data. However, serious comparison with data requires resummation of large endpoint corrections to the color-singlet production cross section. Also, the assumptions underlying our calculations require that we apply our results to data without cuts on p_\perp and diffractive contributions that are commonly used in existing experimental analyses. Resumming color-singlet contribution and relaxing experimental cuts could both lead to more room for color-octet contributions in a complete analysis of J/ψ photoproduction near $z \rightarrow 1$.

Acknowledgments

A.L. was supported in part by the National Science Foundation under Grants No. PHY-0244599 and PHY-0546143. Adam Leibovich is a Cottrell Scholar of the Research Corporation. T.M. was supported in part by the Department of Energy under grant numbers DE-FG02-96ER40945 and DE-AC05-84ER40150.

APPENDIX A

Here we derive Eqs. (48) and (49). We aim to extract terms that are singular as $z \rightarrow 1$, so we will systematically drop all contributions which are regular in this limit. We start with Eq. (48):

$$(1-z)^{-1-\epsilon} \int_0^z dx \frac{(z-x)^{-\epsilon}}{1-x} g(x) = \tag{A1}$$

$$(1-z)^{-1-\epsilon} \left[g(1) \int_0^z dx \frac{(z-x)^{-\epsilon}}{1-x} + \int_0^z dx \frac{(z-x)^{-\epsilon}}{1-x} (g(x) - g(1)) \right].$$

We assume $g(x)$ can be expanded about $x = 1$. To evaluate the second term on the right hand side of Eq. (A1), we note the distributional identity in Eq. (38) implies

$$(1-z)^{-1-\epsilon} f(z) = (1-z)^{-1-\epsilon} f(1) + \dots, \tag{A2}$$

where the ellipsis denotes terms that are not nonsingular as $z \rightarrow 1$ for any function $f(z)$ which can be expanded about $z = 1$. The integral in the second term can therefore be evaluated with $z = 1$:

$$(1-z)^{-1-\epsilon} \int_0^z dx \frac{(z-x)^{-\epsilon}}{1-x} (g(x) - g(1)) \tag{A3}$$

$$= (1-z)^{-1-\epsilon} \int_0^1 dx (1-x)^{-1-\epsilon} (g(x) - g(1))$$

$$= (1-z)^{-1-\epsilon} \int_0^1 dx \left[\left(\frac{1}{1-x} \right)_+ - \epsilon \left(\frac{\ln(1-x)}{1-x} \right)_+ \right] g(x).$$

We can use the distributional identity in Eq. (38) and expand in ϵ to obtain

$$(1-z)^{-1-\epsilon} \int_0^z dx \frac{(z-x)^{-\epsilon}}{1-x} (g(x) - g(1)) = \tag{A4}$$

$$\delta(1-z) \left[-\frac{1}{\epsilon} \int_0^1 dx \left(\frac{1}{1-x} \right)_+ g(x) + \int_0^1 dx \left(\frac{\ln(1-x)}{1-x} \right)_+ g(x) \right]$$

$$+ \left(\frac{1}{1-z} \right)_+ \int_0^1 dx \left(\frac{1}{1-x} \right)_+ g(x).$$

To evaluate the first integral on the right hand side of Eq. (A1) we remember that

$$(1-z)^{-1-\epsilon} \int_0^z dx \frac{(z-x)^{-\epsilon}}{1-x}$$

is really a distribution so we consider the double integral:

$$I = \int_0^1 dz f(z) (1-z)^{-1-\epsilon} \int_0^z dx \frac{(z-x)^{-\epsilon}}{1-x},$$

where $f(z)$ is a smooth function. Writing I as

$$I = \int_0^1 dz [f(z) - f(1)] (1-z)^{-1-\epsilon} \int_0^z dx \frac{(z-x)^{-\epsilon}}{1-x}$$

$$+ f(1) \int_0^1 dz (1-z)^{-1-\epsilon} \int_0^z dx \frac{(z-x)^{-\epsilon}}{1-x},$$

we see that the integrand of the first term is finite as $z \rightarrow 1$ so we can set $\epsilon \rightarrow 0$ in evaluating this term. The second term is straightforward to evaluate after interchanging the order of the x and z integrations. The result is

$$\begin{aligned} I &= - \int_0^1 dz [f(z) - f(1)] \frac{\ln(1-z)}{1-z} - f(1) \frac{1}{2\epsilon} \frac{\Gamma[-\epsilon]\Gamma[1-\epsilon]}{\Gamma[1-2\epsilon]} \\ &= \int_0^1 dz f(z) \left[\delta(1-z) \left(\frac{1}{2\epsilon^2} - \frac{\pi^2}{12} \right) - \left(\frac{\ln(1-z)}{1-z} \right)_+ \right], \end{aligned} \quad (\text{A5})$$

so we obtain the distributional identity

$$(1-z)^{-1-\epsilon} \int_0^z dx \frac{(z-x)^{-\epsilon}}{1-x} = \delta(1-z) \left(\frac{1}{2\epsilon^2} - \frac{\pi^2}{12} \right) - \left(\frac{\ln(1-z)}{1-z} \right)_+. \quad (\text{A6})$$

Combining Eq.(A1), Eq.(A6), and Eq.(A4) yields the result in Eq. (48).

To obtain the result in Eq. (49), we first note that we can replace $g(x)$ with $g(1)$ and then use

$$\begin{aligned} &\int_0^1 dz f(z) (1-z)^{-\epsilon} \int_0^z dx \frac{(z-x)^{-\epsilon}}{(1-x)^2} \\ &= \int_0^1 dz [f(z) - f(1)] \int_0^z dx \frac{1}{(1-x)^2} + f(1) \int_0^1 dz (1-z)^{-\epsilon} \int_0^z dx \frac{(z-x)^{-\epsilon}}{(1-x)^2} \\ &= \int_0^1 dz f(z) \left[-\frac{1}{2\epsilon} \delta(1-z) + \left(\frac{1}{1-z} \right)_+ \right], \end{aligned} \quad (\text{A7})$$

plus nonsingular terms.

APPENDIX B

Here we discuss zero-bin subtractions in more detail and show how they can be implemented at the level of the Lagrangian by introducing a fictitious field. A collinear particle is defined in SCET by rephrasing the full theory fields:

$$\phi(x) = \sum_{\vec{p} \neq 0} e^{-i\vec{p} \cdot \vec{x}} \phi_{\vec{p}}(x). \quad (\text{B1})$$

Loop integrals as well as phase space integrations involve both a sum over labels and an integral over residual momentum which can be performed using the following trick:

$$\sum_{\vec{p}} \int d^D k = \int d^D p, \quad (\text{B2})$$

which allows one to avoid doing explicit sums in loops and in phase space. Note that the sums in Eq. (B1) and Eq. (B2) differ. In defining the fields, we only include nonvanishing label momentum, $\vec{p} \neq 0$, since when the label momentum vanishes the particle should really be regarded as ultrasoft. However, the trick in Eq. (B2) requires that the sum include the

so-called “zero-bin”, the momentum region with vanishing label momentum $\vec{p} = 0$. Careful evaluation of the sum over labels and integrals requires modifying Eq. (B2) [27]:

$$\sum_{\vec{p} \neq 0} \int d^D k F[p, k] = \int d^D p (F[p] - \text{subtraction}) . \quad (\text{B3})$$

In a tree level calculation which involves phase space integrals, one can deal with the zero-bin by putting a cutoff in the phase space integral that separates the integration region into $x - z \sim O(\lambda^2)$ and $x - z \sim O(1)$ regions, and only use the appropriate mode in the respective regions. This is somewhat clumsy and a more elegant way to achieve the desired result is to extend both the collinear and soft particle diagrams to cover the entire phase space and introduce a fictitious particle, ϕ^{zb} , which cancels off the double counting in the corner of phase where such a cancellation is needed. We modify the definition of the collinear field so the sum is over all labels but the contribution of the spurious zero-mode is cancelled by a fictitious degree of freedom:

$$\phi(x) = \sum_{\vec{p}} e^{-i\vec{p}\cdot\vec{x}} \phi_{\vec{p}}(x) - \phi^{zb}(x) . \quad (\text{B4})$$

If we use the fictitious ϕ^{zb} field then we can convert sums over labels ordinary loop integrals and phase space integrals using Eq. (B2) but there are extra diagrams with the zero-bin field which cancel spurious zero-bin contributions in the collinear graphs. These fields have the same couplings as collinear fields but their diagrams contribute with opposite sign and they have vanishing label momentum. Evaluating real emission graphs with ϕ^{zb} yields Eq. (60).

-
- [1] W. E. Caswell and G. P. Lepage, Phys. Lett. B **167**, 437 (1986).
 - [2] G. T. Bodwin, E. Braaten and G. P. Lepage, Phys. Rev. D **51**, 1125 (1995). [Erratum-ibid. D **55**, 5853 (1995)].
 - [3] M. E. Luke, A. V. Manohar and I. Z. Rothstein, Phys. Rev. D **61**, 074025 (2000).
 - [4] R. Barbieri, R. Gatto and E. Remiddi, Phys. Lett. B **61**, 465 (1976); Phys. Lett. B **106**, 497 (1981); R. Barbieri, M. Caffo, R. Gatto and E. Remiddi, Nucl. Phys. B **192**, 61 (1981).
 - [5] G. T. Bodwin, E. Braaten and G. P. Lepage, Phys. Rev. D **46**, 1914 (1992).
 - [6] E. Braaten and S. Fleming, Phys. Rev. Lett. **74**, 3327 (1995).
 - [7] P. L. Cho and A. K. Leibovich, Phys. Rev. D **53**, 150 (1996); Phys. Rev. D **53**, 6203 (1996).
 - [8] A. A. Affolder *et al.* [CDF Collaboration], Phys. Rev. Lett. **85**, 2886 (2000).
 - [9] M. Cacciari and M. Kramer, Phys. Rev. Lett. **76**, 4128 (1996).
 - [10] P. Ko, J. Lee and H. S. Song, Phys. Rev. D **54**, 4312 (1996) [Erratum-ibid. D **60**, 119902 (1999)].
 - [11] M. Cacciari, M. Greco, M. L. Mangano and A. Petrelli, Phys. Lett. B **356**, 553 (1995).
 - [12] M. Beneke and M. Kramer, Phys. Rev. D **55**, 5269 (1997).
 - [13] B. A. Kniehl and G. Kramer, Eur. Phys. J. C **6**, 493 (1999).
 - [14] E. Braaten, B. A. Kniehl and J. Lee, Phys. Rev. D **62**, 094005 (2000).
 - [15] B. Cano-Coloma and M. A. Sanchis-Lozano, Nucl. Phys. B **508**, 753 (1997).
 - [16] S. P. Baranov, Phys. Rev. D **66**, 114003 (2002).
 - [17] B. A. Kniehl and G. Kramer, Phys. Rev. D **56**, 5820 (1997).

- [18] B. A. Kniehl and G. Kramer, Phys. Lett. B **413**, 416 (1997).
- [19] M. Beneke, I. Z. Rothstein and M. B. Wise, Phys. Lett. B **408**, 373 (1997).
- [20] M. Beneke, G. A. Schuler and S. Wolf, Phys. Rev. D **62**, 034004 (2000).
- [21] S. Fleming, A. K. Leibovich and T. Mehen, Phys. Rev. D **68**, 094011 (2003).
- [22] C. W. Bauer, S. Fleming and M. Luke, Phys. Rev. D **63**, 014006 (2001).
- [23] C. W. Bauer, S. Fleming, D. Pirjol and I. W. Stewart, Phys. Rev. D **63**, 114020 (2001).
- [24] C. W. Bauer and I. W. Stewart, Phys. Lett. B **516**, 134 (2001).
- [25] C. W. Bauer, D. Pirjol and I. W. Stewart, Phys. Rev. D **65**, 054022 (2002).
- [26] C. W. Bauer, D. Pirjol and I. W. Stewart, Phys. Rev. D **67**, 071502 (2003).
- [27] A. V. Manohar and I. W. Stewart, hep-ph/0605001.
- [28] S. Fleming, A. K. Leibovich and T. Mehen, hep-ph/0512194.
- [29] C. M. Arnesen, J. Kundu and I. W. Stewart, Phys. Rev. D **72**, 114002 (2005).
- [30] C. W. Bauer, S. Fleming, D. Pirjol, I. Z. Rothstein and I. W. Stewart, Phys. Rev. D **66**, 014017 (2002).
- [31] J. Amundson, S. Fleming and I. Maksymyk, Phys. Rev. D **56**, 5844 (1997).
- [32] F. Maltoni, M. L. Mangano and A. Petrelli, Nucl. Phys. B **519**, 361 (1998).
- [33] A. Petrelli, M. Cacciari, M. Greco, F. Maltoni and M. L. Mangano, Nucl. Phys. B **514**, 245 (1998).
- [34] C. W. Bauer, C. W. Chiang, S. Fleming, A. K. Leibovich and I. Low, Phys. Rev. D **64**, 114014 (2001).
- [35] G. Sterman, “An Introduction to Quantum Field Theory,” Cambridge University Press, Cambridge, 1993.
- [36] G. P. Korchemsky and A. V. Radyushkin, Sov. J. Nucl. Phys. **45**, 127 (1987) [Yad. Fiz. **45**, 198 (1987)].
- [37] G. P. Korchemsky and G. Marchesini, Nucl. Phys. B **406**, 225 (1993).
- [38] A. K. Leibovich, I. Low and I. Z. Rothstein, Phys. Rev. D **61**, 053006 (2000).
- [39] A. K. Leibovich, I. Low and I. Z. Rothstein, Phys. Lett. B **513**, 83 (2001).
- [40] S. W. Bosch, R. J. Hill, B. O. Lange and M. Neubert, “Factorization and Sudakov resummation in leptonic radiative B decay,” Phys. Rev. D **67**, 094014 (2003) [arXiv:hep-ph/0301123].
- [41] K. Abe *et al.* [BELLE Collaboration], Phys. Rev. Lett. **88**, 052001 (2002).
- [42] B. Aubert *et al.* [BABAR Collaboration], Phys. Rev. Lett. **87**, 162002 (2001).
- [43] K. Abe *et al.* [Belle Collaboration], Phys. Rev. Lett. **89**, 142001 (2002).
- [44] K. Abe *et al.* [Belle Collaboration], Phys. Rev. D **70**, 071102 (2004)
- [45] P. L. Cho and A. K. Leibovich, Phys. Rev. D **54**, 6690 (1996); S. Baek, P. Ko, J. Lee and H. S. Song, J. Korean Phys. Soc. **33**, 97 (1998).
- [46] A. K. Leibovich, Z. Ligeti and M. B. Wise, Phys. Lett. B **539**, 242 (2002).
- [47] H. L. Lai *et al.* [CTEQ Collaboration], Eur. Phys. J. C **12**, 375 (2000)
- [48] S. Fleming, A. K. Leibovich and T. Mehen, work in progress.
- [49] S. Chekanov *et al.* [ZEUS Collaboration], Eur. Phys. J. C **27**, 173 (2003).